Theoretical studies on structural and decay properties of Z=119 superheavy nuclei

M. Ikram^{1a}, Asloob A. Rather¹, A. A. Usmani¹ Bharat Kumar^{2,3}, S. K. Patra^{2,3}

- Department of Physics, Aligarh Muslim University, Aligarh-202002, India.
- ² Institute of Physics, Bhubaneswar-751 005, India.
- ³ Homi Bhabha National Institute, Anushakti Nagar, Mumbai-400094, India

Received: date / Revised version: date

Abstract. In this manuscript, we analyze the structural properties of Z=119 superheavy nuclei in the mass range of 284 < A < 375 within the framework of axially deformed relativistic mean field theory (RMF) and calculate the binding energy, radii, quadrupole deformation parameter, separation energies and density profile. To investigate the phenomenon of shape coexistence the RMF calculations are performed within three possible solutions i.e. prolate, oblate and spherical configurations. To get a better visualization of nucleon and total matter distribution, two-dimensional contour representation of density distribution for $^{291}119$ and $^{303}119$ has been made. A competition between possible decay modes such as α -decay, β -decay and spontaneous fission (SF) of the isotopic chain of Z=119 is systematically analyzed within self-consistent relativistic mean field model. The α -decay half lives are estimated using the semi-empirical formulae by Viola-Seaborg [V. E. Viola, Jr. and G. T. Seaborg, J. Inorg. Nucl. Chem. 28, 741 (1966)], B. A. Brown [B. A. Brown, Phys. Rev. C 46, 811 (1992)], G. Royer [G. Royer, J. Phys. G, Nucl. Part. Phys. 26, 1149 (2000)], N. Dasgupta-Schubert and M.A. Reyes [N. Dasgupta-Schubert and M.A. Reyes, At. Data Nucl. Data Tables 93, 90 (2007)], D. D. Ni et al., [D.D. Ni, Z. Z. Dong, and T. K et al., Phys. Rev. C, 78, 044310 (2008)] and a close agreement is noticed amongst these and also with the estimations made by Finite Range Droplet Model (FRDM) wherever available. Moreover, our analysis confirmed that α -decay is restricted within the mass range $284 \le A \le 297$ and thus being the dominant decay channel in this mass range. There is no possibility of β -decay for the considered isotopic chain. In addition, we forecasted the α -decay chain of fission survival nuclides i.e. $^{284-297}119$ and found as one α chain from $^{297}119$, two consistent α chains from $^{284,285,296}119$, three consistent α chains from $^{294,295}119$, four consistent α chains from $^{285}119$, five consistent α chains from $^{286}119$, seven consistent alpha chains from $^{287,292,293}119$ and nine consistent alpha chains from ^{288,289,290,291}119. Present findings have great significance to the experimentalists in very near future for synthesizing the isotopes of Z = 119 superheavy nuclei.

PACS. PACS-key discribing text of that key - PACS-key discribing text of that key

1 Introduction

Theoretical and experimental studies of the nuclei with large number of neutrons and protons has witnessed an upsurge and has become the subject of intense debate among nuclear physics community from past several decades Thus, exploring the existence limit of very heavy nuclei, i.e., nuclei with $Z \geq 104$ and island of stability in superheavy nuclei (SHN) has been a challenging issue in nuclear physics from a fairly long period of time. The discovery of new superheavy elements (SHEs) has lead to the simultaneous expansion of periodic table and Segre chart of nuclei. Hence, the studies based on the identification of new SHN would extend our knowledge about the nuclear potentials and resulting nuclear structure. The hunt for SHN started in the late 1960s with the island of stability

around Z = 114 and N = 184 [1]. The existence of superheavy nuclei is the result of the interplay between large disruptive coulomb force and the attractive nuclear potential. Owing to the large number of protons in SHN the coulomb disruption dominates the attract nuclear force thus making the SHN unstable and therefore highly susceptible to spontaneous fission. The question that arise then is what makes these SHN stable. The answer to this question came however by the end of 1960s, when it was firmly established that the existence of heavier nuclei with $Z \geq 104$ was primarily determined by the quantum mechanical shell effects i.e. single-particle motion of neutrons and protons in quantum orbits [2,3,4,5,6]. The next fundamental question that nuclear physics community try to find out is the maximum possible combination of neutrons and proton that can found or synthesized in the laboratory. With the huge progress in theory, ex-

 $^{^{\}mathrm{a}}$ e-mail:ikramamu@gmail.com

periments and accelerator technologies and the advent of state-of-art radioactive ion beam facilities, it has become possible to synthesize the superheavy nuclei and reach to the island of stability in superheavy nuclei. The process of synthesizing SHN is done via fusion evaporation reactions, i.e. cold fusion reaction [7] and hot fusion reaction [8]. The cold fusion technique which involves doubly magic spherical target and deformed projectile has been successful in synthesizing Z = 107 - 113 [9, 10, 11] at GSI, Darmstadt and RIKEN Japan. On the other hand hot fusion reaction using neutron-rich ⁴⁸Ca beams on actinide targets, the synthesis of Z = 107 - 118 have been done at JINR-FLNR, Dubna [12]. Recently in 2009, an attempt to synthesis Z = 120 by using hot fusion reaction was made by Oganessian et al. [13]. However, due to the low cross-section values of the order of picobarn and sub-picobarn levels obtained in the experiments for synthesizing SHN makes the experiment to last for several months and henceforth results in the identification of few events(nuclei). Analysis of low-statistics data and investigation of new isotopes becomes of crucial importance. Thus, running of experiments for long periods results in optimization of production methods through the determination of excitation functions as demonstrated in recent studies of the $^{232}Am+^{48}Ca$ reaction [14,15].

The elusive superheavy mass region provide an opportunity to nuclear physicists to explore the concepts like magic numbers and island of stability, which help us to understand why certain nuclei are more stable than others. Various theoretical investigations have been carried using microscopic-macroscopic approaches and the self-consistent mean-field in both the relativistic and nonrelativistic domains [16,17] and the primary goal of these studies is to find out the combination of neutrons and protons where spherical shell closure may occur. However, there is no general consensus among relativistic and nonrelativistic theoretical models in predicting spherical shell closures. For instance, the nuclear shell model predicts the next magic number beyond Z = 82 at Z = 114. However, the microscopic-macroscopic model predicts it to be at Z = 114 and N = 184 [18, 19, 20] which is considered to be the island of superheavy mass region and confirmation of it has become a much debated issue nowadays. There is no confirmation till date regarding the center of island of stability in SHN. Analogues to mic-mac predictions, the microscopic models predicts closed spherical shell closures at N = 184 but for nuclei with higher number of protons, i.e., Z = 120, 122, 124 or 126 [1, 21, 22, 23, 24, 25, 26]. However, it is to be noted that most of the theoretical investigations predict N = 184 as the neutron magic number. The fragility/uncertainty in predicting the correct proton magic number is attributed to the ambiguous strength of spin orbit coupling which posses a great difficulty in localization of single-particle energy levels between Z = 114and 126.

The theoretical investigations carried out specifically on α -decay properties in superheavy mass have close connection to the nuclear model predictions [27,28,29] like clustering, shell structures, deformations and quasi-particle

excitations and various theoretical approaches have been put forth for computation of α -decay properties in the superheavy mass region. One of the effective ways possibly to study SHNs is via the characterizations of their decay properties and in particular α -decay is considered to be an inevitable tool to identify and study SHN as it provides world of information regarding the nuclear structure. The prominent mode of decay in superheavy mass region is alpha decay followed by spontaneous fission. The proper measurement of alpha decay properties provide useful inputs on structure of superheavy nuclei, for instance, shell effects and stability, nuclear spins and parities, deformation, rotational properties, fission barrier, etc. The credit to the discovery of α -decay goes to Rutherford [30,31] in 1899 and Gamow [32] was first to describe it in 1928 using the concept of quantum tunnelling through potential barrier. Currently various theoretical investigations which belong to macro-micro methods like the cluster model [33], fission model [34], the density dependent M3Y (DDM3Y) effective model [35], the generalized liquid drop model(GLDM) [36], etc and the self-consistent models like relativistic mean-field theory [17], Skyrme-Hartree-Fock mean field model [37] are being employed to explain the α -decay from heavy and superheavy nuclei. Recently, working within the ambit of axially deformed relativistic mean field model by employing NL3* parameterization, a systematic study of alpha decay half lives of predicted magic nuclei Z = 132, 138 [38] in the mass range 312 < A < 392 has been made and computation of alpha decay half lives was performed by using the semi-empirical formulae VSS [39], Brown [41], Royer [40], GLDM [42] and Ni et al., [43]. By employing 20 mass models and 18 empirical formulae an extensive and systematic study was performed by Wang et al. [44] on alpha decay energies and alpha decay half lives of superheavy nuclei with $Z \geq 100$ respectively and established that for reproducing the Q_{α} values of SHN, the WS4 mass model is most appropriate one. Moreover, the outcome of these studies firmly authorized that out of 18 empirical formulae SemFIS2 [45] is the most reliable one to predict alpha decay half lives as the parameters involved in the formula are taken from experimental alpha emitter data of transuranium nuclei including SHN(Z = 92 - 118) and the UNIV2 [45] formulae with fewest parameters is also effective in superheavy mass region. Moreover, VSS [46, 47, SP [48,49] and NRDX [50] employing fewer parameters are also very handy in the prediction of alpha decay half lives.

Although both alpha decay and spontaneous fission are explained by quantum mechanical tunnelling, the two widely differ in principle. Whereas alpha decay is described as the alpha cluster penetrating the coulomb barrier after its formation in the parent nucleus, the process of spontaneous fission is much more intricate as it involves large uncertainties such as mass and charge numbers of the two fragments, the number of emitted neutrons, and the released energy etc. It is to be emphasized that though alpha decay and spontaneous fission are the principal modes of decay of superheavy nuclei with $Z \geq 92$, it the spon-

taneous fission that acts as limiting factor for determining the stability of superheavy nuclei. In 1939 Bohr and Wheeler [51] described the mechanism of spontaneous fission and established a limit $\frac{Z^2}{A} \approx 48$ for SF beyond which nuclei are susceptible to spontaneous fission. Flerov et al. [52] observed SF from ²³⁸U and this was followed by several empirical formulae being proposed for determining the SF half lives and it was Swatecki [53] in 1955 who put forward the first semi-empirical formulae for estimation of SF half lives. Presently, we come across the globe in different laboratories [54,55,56,57,58,59] SF half lives being measured and extensive theoretical investigations carried out by several theoretical groups for identifying the long lived superheavy elements. Several empirical formulae have been proposed for estimation of SF fission half lives by different researchers. Xu et al. [60] put forward a semi-empirical formula for estimating SF half life of even-even nuclei using parabolic potential and the agreement between theoretical and experimental results is quite good. A phenomenological formula proposed by Ren et al. [61,62] in 2005 for calculating SF half lives of eveneven nuclei was generalized to both the case of odd nuclei and fission isomers. Within the microscopic-macroscopic model approach, Smolanczuk et al. [63] calculated the SF properties for deformed even-even, odd-A and odd-odd superheavy nuclei with Z = 104 - 120. This was followed by computation of spontaneous fission barriers of Z = 96120 by Muntain et al. [64] within microscopic-macroscopic model. By employing Hartree-Fock-Bogoliubov(HFB) approach with finite range and density dependent Gogny force with the DIS parameter set Warda et al. [65] estimated the SF half lives of 160 heavy and superheavy nuclei. The study carried out by Stasczak et al. [66] by using density functional theory for estimation of SF half lives and life times of superheavy elements presented a systematic self-consistent approach to SF in SHN. The computation of SF half lives using the semi-empirical formula by Ren and Xu for Z = 132, 138 with mass ranges $312 \le A \le 392$ and $318 \le A \le 398$ has been done recently and reported in Ref. [38]. In present manuscript, our main motive is to investigate the decay properties of isotopes of Z = 119 superheavy nuclei that would hopefully be quite useful for experimental point of view. In this view, we made an attempt to analyze the competition among various possible modes of decay of Z = 119 superheavy nuclei such as α -decay, β -decay and SF along with the structural studies and predict the principal mode of decay of considered isotopic chain. Further, we performed the study about feasibility of observing the α -decay chains for fission survival nuclides i.e. ^{284–297}119 of the considered isotopic chain. The contents of the manuscript are organized as follows: The framework of relativistic meanfield formalism is outlined in section two. Results and discussion is presented in section three. Finally, section four contains the main summary and conclusions of this work.

2 Theoretical Formalism

From last few decades, the relativistic mean field theory has been successfully reproduced the ground state energy and other physical observables of the nuclei throughout the periodic table near as well as far from the stability line including superheavy valley [67,68,69,70,71,72, 73,74,75]. The starting point of the RMF theory is the basic Lagrangian density containing nucleons interacting via exchange of σ -, ω - and ρ -mesons. The contribution of π -meson is zero at mean field due to its pseudo scalar nature. Thus, σ -, ω - and ρ - are only the mesonic field in which σ -, ω - mesons reproduce the large scalar and vector potentials and as a result originate the reasonable nuclear mean potential and large spin-orbit potential. The ρ -meson takes the care of nuclear asymmetry of the systems. Moreover, photon field A_{μ} is included to handle the Coulomb interaction between protons. The relativistic mean field Lagrangian density is expressed as [67,68,69,

$$\mathcal{L} = \bar{\psi}_i \{ i \gamma^{\mu} \partial_{\mu} - M \} \psi_i + \frac{1}{2} \partial^{\mu} \sigma \partial_{\mu} \sigma - \frac{1}{2} m_{\sigma}^2 \sigma^2 - \frac{1}{3} g_2 \sigma^3
- \frac{1}{4} g_3 \sigma^4 - g_{\sigma} \bar{\psi}_i \psi_i \sigma - \frac{1}{4} \Omega^{\mu\nu} \Omega_{\mu\nu} + \frac{1}{2} m_w^2 V^{\mu} V_{\mu}
- g_w \bar{\psi}_i \gamma^{\mu} \psi_i V_{\mu} - \frac{1}{4} \mathbf{B}^{\mu\nu} \mathbf{B}_{\mu\nu} + \frac{1}{2} m_{\rho}^2 \mathbf{R}^{\mu} \mathbf{R}_{\mu} - \frac{1}{4} F^{\mu\nu} F_{\mu\nu}
- g_{\rho} \bar{\psi}_i \gamma^{\mu} \boldsymbol{\tau} \psi_i \mathbf{R}^{\mu} - e \bar{\psi}_i \gamma^{\mu} \frac{(1 - \tau_{3i})}{2} \psi_i A_{\mu}. \tag{1}$$

Here M, m_{σ} , m_{ω} and m_{ρ} are the masses for nucleon, $\sigma-$, $\omega-$ and $\rho-$ mesons and ψ is its Dirac spinor. The field for the $\sigma-$ meson is denoted by σ , $\omega-$ meson by V_{μ} and $\rho-$ meson by R_{μ} . The quantities g_{σ} , g_{ω} , g_{ρ} and $e^2/4\pi=1/137$ are the coupling constants for the $\sigma-$, $\omega-$, $\rho-$ mesons and photon field respectively. The g_2 and g_3 are the nonlinear self-interaction coupling constants for $\sigma-$ mesons. By using the classical variational principle, we obtain the field equations for the nucleons and mesons known by Dirac and Klein-Gordon equations. The Dirac equation for the nucleons is written by

$$\{-i\alpha \nabla + V(r_{\perp}, z) + \beta M^{\dagger}\}\psi_i = \epsilon_i \psi_i.$$
 (2)

The effective mass of the nucleon is

$$M^{\dagger} = M + S(r_{\perp}, z) = M + g_{\sigma}\sigma(r_{\perp}, z), \tag{3}$$

and the vector potential is

$$V(r_{\perp}, z) = g_{\omega} V^{0}(r_{\perp}, z) + g_{\rho} \tau_{3} R^{0}(r_{\perp}, z) + e \frac{(1 - \tau_{3})}{2} A^{0}(r_{\perp}, z).$$
(4)

Further, the Klein-Gordon equations are written like as

$$\{-\triangle + m_{\sigma}^{2}\}\sigma^{0}(r_{\perp}, z) = -g_{\sigma}\rho_{s}(r_{\perp}, z) - g_{2}\sigma^{2}(r_{\perp}, z) - g_{3}\sigma^{3}(r_{\perp}, z),$$
(5)

$$\{-\triangle + m_{\omega}^2\} V^0(r_{\perp}, z) = g_{\omega} \rho_v(r_{\perp}, z),$$
 (6)

$$\{-\triangle + m_{\rho}^{2}\}R^{0}(r_{\perp}, z) = g_{\rho}\rho_{3}(r_{\perp}, z),$$
 (7)

$$-\triangle A^{0}(r_{\perp}, z) = e\rho_{c}(r_{\perp}, z). \tag{8}$$

Here $\rho_s(r_{\perp}, z)$, and $\rho_v(r_{\perp}, z)$ are the scalar and vector density for σ - and ω -fields in nuclear system which are expressed as

$$\rho_s(r_{\perp}, z) = \sum_{i=n, p} \bar{\psi}_i(r)\psi_i(r) ,$$

$$\rho_v(r_{\perp}, z) = \sum_{i=n, p} \psi_i^{\dagger}(r)\psi_i(r) .$$
(9)

The vector density $\rho_3(r_{\perp}, z)$ for ρ -field and charge density $\rho_c(r_{\perp}, z)$ are expressed by

$$\rho_3(r_{\perp}, z) = \sum_{i=n,p} \psi_i^{\dagger}(r) \gamma^0 \tau_{3i} \psi_i(r) ,$$

$$\rho_c(r_{\perp}, z) = \sum_{i=n,p} \psi_i^{\dagger}(r) \gamma^0 \frac{(1 - \tau_{3i})}{2} \psi_i(r) .$$
 (10)

A static solution is obtained from the equations of motion to describe the ground state properties of nuclei. The set of nonlinear coupled equations are solved self-consistently in an axially deformed harmonic oscillator basis $N_F = N_B = 20$ and we obtain all the physical observables. The quadrupole deformation parameter β_2 is extracted from the calculated quadrupole moments of neutrons and protons through

$$Q = Q_n + Q_p = \sqrt{\frac{16\pi}{5}} (\frac{3}{4\pi} A R^2 \beta_2), \tag{11}$$

where $R = 1.2A^{1/3}$.

The various rms radii are defined as

$$\langle r_p^2 \rangle = \frac{1}{Z} \int r_p^2 d^3 r \rho_p(r_\perp, z) ,$$

$$\langle r_n^2 \rangle = \frac{1}{N} \int r_n^2 d^3 r \rho_n(r_\perp, z) ,$$

$$\langle r_m^2 \rangle = \frac{1}{A} \int r_m^2 d^3 r \rho(r_\perp, z) ,$$
(12)

for proton, neutron and matter rms radii, respectively. The quantities $\rho_p(r_\perp,z)$, $\rho_n(r_\perp,z)$ and $\rho(r_\perp,z)$ are their corresponding densities. The charge rms radius can be found from the proton rms radius using the relation $r_c = \sqrt{r_p^2 + 0.64}$ by taking finite size of proton into consideration. The total energy of the system is given by

$$E_{total} = E_{part} + E_{\sigma} + E_{\omega} + E_{\rho} + E_{c} + E_{pair} + E_{c.m.}, (13)$$

where E_{part} is the sum of the single particle energies of the nucleons and E_{σ} , E_{ω} , E_{ρ} , E_{c} , E_{pair} , E_{cm} are the contributions of the meson fields, the Coulomb field, pairing energy and the center-of-mass energy, respectively. In present calculations, we use the constant gap BCS approximation to take care of pairing interaction [76]. The parameter set NL3 [77] is used throughout the calculations.

3 Results and discussions

It is worth mentioning that till now the superheavy nuclei up to Z = 118 [78,79] have been synthesized in the laboratory and experiments have also been attempted for the

production of Z = 120 [13], however its production crosssection is very small. Thus, situation demands to choose a proper combination of projectile and target in hot fusion reaction to improve the production cross-section for magic proton shell nuclei (i.e. Z=120). On theoretical estimation of evaporation residue cross-section, many of the possibilities of hot fusion reactions are suggested regarding the synthesization of nuclei with Z = 120 [80,82,83, 81]. Not only this, evaporation residue cross-section for superheavy nuclei with Z = 119 has also been predicted by number of people [82,83,81,84] and some of them found that this nucleus might be produced easier than magic proton shell nuclei [85]. Therefore, experiment to produce isotopes of Z = 119 using hot fusion reactions is of great interest and would bridge the gap between experimentally known Z = 118 and magic proton shell nuclei. Regarding the observation of SHN, it is noticed that the superheavy nuclei are identified by α -decay in the laboratory followed by spontaneous fission. In this view, it make sense to have some theoretical predictions on decay channels of Z=119superheavy nuclei for guiding the experiment. Concerning to this, we make mean field calculations to analyze the competition among α -decay, β -decay and spontaneous fission for predicting the possible mode of decay of isotopic chain under study and this is considered to be central theme of the paper. In addition to gain some structural information, we calculate the total binding energy (BE), radii, quadrupole deformation parameter (β_2) and density profile for three possible shape configurations in the mass range of 284 < A < 375 which covers many of the predicted neutron magic numbers. The results concerning to structure and decay of Z = 119 isotopic chain are fully explained in subsections 3.1 to 3.5.

3.1 Binding energy, radii and quadrupole deformation parameter

The calculated binding energy, radii and quadrupole deformation parameter for the isotopic chain $^{284-375}119$ are given in Tables 1, 2 and plotted in Figures 1, 2. To identify the possible ground state configuration of the nuclei, the field equations are solved with an initial spherical, prolate and oblate quadrupole deformation parameter β_0 in relativistic mean field formalism. Nucleus, a quantum many body system, acquires different binding energy by their possible shape configurations leading to the ground as well as intrinsic excited states. It is worthy to mention that maximum binding energy of a quantum system corresponds to the ground state energy of the system and all other solutions may correspond to the intrinsic excited states. Concerning these facts into consideration, we found prolate as a ground state for most of the nuclides of Z=119. Thus, structural properties and decay energies are plotted and estimated for prolate shaped throughout the chain. Moreover, some nuclides do not have all three well defined shape and we obtain only two solutions of the field equations. As the experimental informations of these isotopes are not available, so in order to provide some validity to the predictive power of our model and their

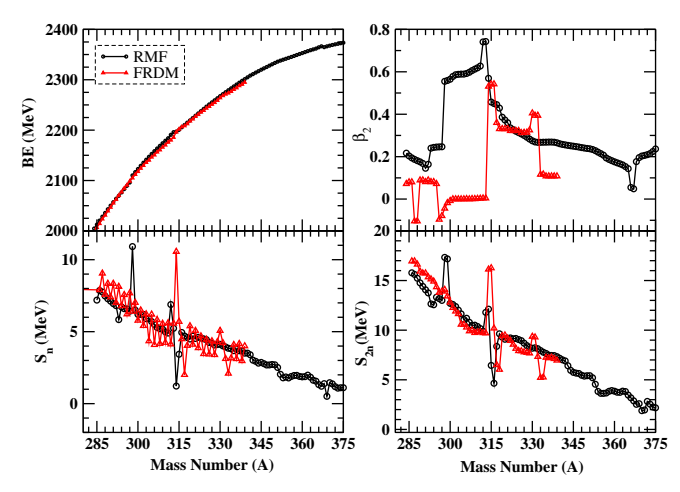


Fig. 1. (color online) Binding energy, quadrupole deformation parameter, one and two-neutron separation energy are given as function of mass number.

results a comparison of binding energies of our calculations with those obtained from finite range droplet model (FRDM) [86] is made wherever available and some how close agreement is found among them. From Table 1, we can see that the binding energy difference between RMF and FRDM is very small. The maximum difference between RMF and FRDM values is about 7 MeV, namely, the relative differences are less than 0.35%. Our calculated one- and two-neutron separation energy is also matches well with FRDM estimations. However, there is no close connection in quadrupole deformation parameter within RMF and the values obtained from FRDM data [86]. Some of the nuclides of considered isotopic series, for example $^{298-318}119$ having large prolate quadrupole deformation parameter and therefore supposed to be superdeformed by their shape. Superdeformation is common phenomenon in RMF calculations and it plays a significant role for stability of superheavy nuclei. The radii increases with increasing the mass number and a sudden change in radii indicates the change in shape of the nuclides. In general, the calculated binding and separation energies from RMF are in good agreement with those of the FRDM values wherever available.

3.2 Neutron-separation energy

Separation energy is the first prime signature to identify the magic behaviour of the nuclei. The magic numbers in nuclei are characterized by large shell gaps in their single-particle energy levels. Large shell gap means the nucleons occupying the lower energy level have comparatively large value of energy than those nucleons occupying the higher energy levels. This large energy difference between two consecutive energy levels can be observed from the sudden fall of neutron separation energy which attribute the extra stability to a particular nucleus having certain numbers of nucleons and that's why closed shell nuclei are more bound

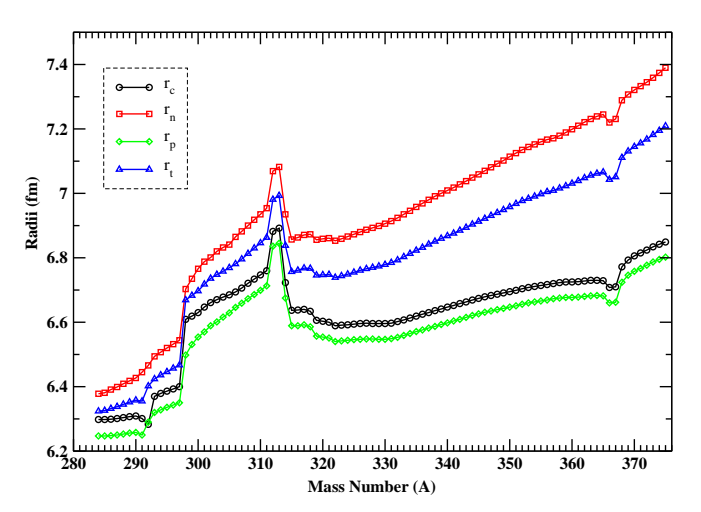


Fig. 2. (color online) Radii as a function of mass number.

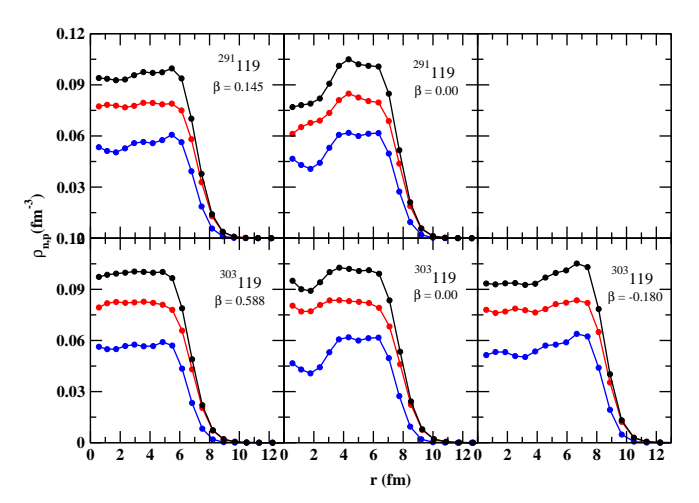


Fig. 3. (color online) Total, neutron and proton density distribution as a function of radial parameter for three possible shape configurations. Lines with black, red and blue colors represent the total, neutron and proton density profile respectively. There is no oblate solution for ²⁹¹119 within the used force parameter set.

than their nearby ones. Moreover, two-neutron separation energy is more significant than one neutron due to its takes care of even-odd staggering and it, therefore, manifests the magicity more clearly. One and two-neutron separation energy is calculated by the difference in binding energies of two isotopes using the relations

$$S_n(N,Z) = BE(N,Z) - BE(N-1,Z),$$

 $S_{2n}(N,Z) = BE(N,Z) - BE(N-2,Z).$ (14)

One- and two-neutron separation energy for the considered isotopic series of the nuclei ^{284–375}119 are plotted in lower panel of Fig. 1. No sudden fall of the separation energies is noticed in present analysis which indicates that

Table 1. Binding energy (BE), quadrupole deformation parameter (β_2) and radii for Z=119 isotopic chain within three possible shape configurations.

Nuclei		BE			β_2			r_c			r_t		FRI	OM
	prol.	sph.	obl.	prol.	sph.	obl.	prol.	sph.	obl.	prol.	sph.	obl.	BE	β_2
284119	2004.6	2002.8		0.217	-0.033		6.298	6.238		6.324	6.263		1997.6	0.072
$^{285}119$	2012.6	2011.9		0.203	-0.068		6.298	6.248		6.326	6.276		2006.6	0.080
$^{286}119$	2020.4	2020.0		0.194	0.045		6.299	6.252		6.332	6.283		2014.5	0.080
$^{287}119$	2028.2	2028.4		0.187	0.039		6.301	6.257		6.338	6.292		2023.6	-0.104
²⁸⁸ 119	2035.7	2036.7		0.181	0.018		6.304	6.262		6.345	6.301		2031.1	-0.104
²⁸⁹ 119	2042.9	2044.9		0.175	-0.002		6.307	6.268		6.352	6.310		2039.5	0.089
$^{290}_{201}119$	2050.1	2052.9		0.168	-0.001		6.309	6.274		6.358	6.319		2046.9	0.089
²⁹¹ 119	2057.0	2060.6		0.145	-0.001		6.301	6.279		6.355	6.328		2055.2	0.081
²⁹² 119	2063.8	2067.8	2066.2	0.163	-0.001	-0.165	6.317	6.283	6.312	6.375	6.337	6.366	2062.2	0.089
$^{293}_{294}119$	2069.6	2074.6	2073.6	0.240	-0.001	-0.172	6.370	6.286	6.322	6.424	6.345	6.378	2070.4	0.081
$^{295}119$	2076.4	2081.1	2080.4	0.243	-0.001	-0.178	6.379	6.290	6.330	6.436	6.353	6.390	2077.2	0.081
$^{296}119$	2083.0 2089.5	2087.6 2094.0	2087.2 2094.2	$0.245 \\ 0.246$	-0.002 -0.001	-0.222 -0.237	6.386 6.393	6.293 6.296	6.364 6.381	$6.446 \\ 6.457$	$6.361 \\ 6.369$	6.423 6.443	2084.7 2090.9	0.072 -0.096
$^{297}119$	2089.3	2094.0 2100.4	2101.0	0.240 0.247	-0.001	-0.244	6.400	6.299	6.392	6.467	6.377	6.445	2090.9	-0.079
$^{298}119$	2110.2	2106.4	2107.5	0.247 0.555	-0.001	-0.244 -0.251	6.609	6.302	6.403	6.669	6.385	6.471	2098.0 2105.0	-0.044
$^{299}119$	2116.7	2113.1	2113.7	0.559	-0.001	-0.259	6.619	6.305	6.415	6.683	6.393	6.486	2112.0	-0.018
$^{300}119$	2122.9	2119.4	2119.8	0.565	0.000	-0.266	6.630	6.308	6.427	6.697	6.401	6.501	2117.8	-0.008
$^{301}119$	2129.1	2125.5	2125.8	0.578	0.000	-0.273	6.647	6.311	6.438	6.718	6.410	6.515	2124.3	0.000
$^{302}119$	2135.3	2131.5	2130.2	0.586	0.000	-0.180	6.661	6.315	6.378	6.736	6.418	6.467	2129.7	0.000
$^{303}119$	2141.2	2137.1	2136.1	0.588	0.000	-0.180	6.670	6.320	6.384	6.748	6.427	6.477	2135.9	0.000
$^{304}119$	2147.1	2142.5	2141.8	0.589	0.000	-0.183	6.678	6.326	6.392	6.758	6.437	6.488	2140.3	0.000
$^{305}119$	2152.8	2147.6	2147.3	0.589	0.000	-0.188	6.685	6.333	6.401	6.769	6.448	6.500	2146.5	0.000
$^{306}119$	2158.3	2152.5	2152.6	0.592	0.000	-0.194	6.694	6.342	6.412	6.781	6.459	6.513	2150.6	0.001
$^{307}119$	2163.6	2157.4	2158.0	0.598	-0.001	-0.201	6.706	6.351	6.422	6.796	6.470	6.526	2156.4	0.000
$^{308}_{300}$ 119	2168.8	2162.3	2163.3	0.606	0.012	-0.208	6.721	6.360	6.433	6.813	6.481	6.540	2160.6	0.001
³⁰⁹ 119	2174.0	2167.4	2168.5	0.613	0.030	-0.214	6.734	6.370	6.443	6.830	6.493	6.553	2166.1	0.001
³¹⁰ 119	2178.9	2172.4	2173.6	0.619	0.039	-0.218	6.747	6.380	6.452	6.846	6.505	6.566	2170.4	0.002
$^{311}119$ $^{312}119$	2183.9	2177.4	2178.6	0.627	0.043	-0.223	6.760	6.390	6.462	6.863	6.517	6.578	2176.0	0.003
³¹³ 119	2190.7	2182.4	2183.5	0.741	0.044	-0.227	6.882	6.399	6.506	6.981	6.528	6.591	2180.1	0.004
$^{314}119$	2196.0 2197.2	2187.2 2192.0	2188.2 2193.0	0.743 0.569	$0.042 \\ 0.035$	-0.233 -0.240	6.892 6.723	$6.408 \\ 6.416$	6.483 6.494	6.993 6.838	6.539 6.549	6.605 6.619	2185.7 2196.3	$0.004 \\ 0.531$
$^{315}119$	2200.6	2192.0	2193.0	0.309 0.458	0.000	-0.240 -0.247	6.637	6.425	6.506	6.757	6.559	6.633	2190.5 2202.0	0.531 0.541
$^{316}119$	2205.6	2201.6	2202.4	0.450	0.000	-0.247	6.638	6.434	6.517	6.761	6.570	6.648	2206.4	0.541 0.542
$^{317}119$	2210.3	2206.3	2207.1	0.445	0.000	-0.259	6.640	6.442	6.527	6.768	6.580	6.661	2208.5	0.360
$^{318}119$	2214.9	2210.6	2211.7	0.429	0.000	-0.264	6.634	6.449	6.537	6.767	6.591	6.674	2212.5	0.331
$^{319}119$	2219.3	2214.5	2216.3	0.386	0.000	-0.269	6.606	6.456	6.547	6.746	6.601	6.688	2217.9	0.331
$^{320}119$	2224.0	2218.2	2220.7	0.373	0.000	-0.274	6.603	6.462	6.556	6.747	6.610	6.701	2222.0	0.331
$^{321}119$	2228.6	2221.7	2225.3	0.360	0.001	-0.279	6.600	6.468	6.565	6.748	6.620	6.714	2227.0	0.331
$^{322}119$	2233.2		2229.6	0.336		-0.284	6.589		6.573	6.739		6.726	2230.9	0.322
$^{323}119$	2237.7		2231.9	0.328		-0.191	6.591		6.526	6.744		6.682	2235.6	0.322
$\frac{324}{225}$ 119	2242.2		2236.1	0.320		-0.189	6.592		6.532	6.749		6.691	2239.1	0.322
$^{325}_{326}119$	2246.7		2240.4	0.313		-0.189	6.594		6.538	6.755		6.701	2243.5	0.322
	2250.9		2244.4	0.307		-0.191	6.596		6.545	6.761		6.711	2247.0	0.312
$\frac{327}{328}119$	$\begin{array}{c} 2255.1 \\ 2259.2 \end{array}$		$2248.5 \\ 2252.4$	$0.300 \\ 0.292$		-0.195 -0.199	6.597 6.596		$6.552 \\ 6.559$	$6.766 \\ 6.770$		$6.722 \\ 6.733$	$\begin{array}{c} 2251.3 \\ 2254.7 \end{array}$	0.313 0.314
$^{329}119$	2263.3		2252.4 2256.2	0.292		-0.199	6.596		6.566	6.774		6.745	2254.7 2259.0	0.314 0.325
$^{330}119$	2267.4		2260.2 2260.0	0.235 0.275		-0.204	6.596		6.574	6.779		6.757	2264.1	0.325 0.405
$^{331}119$	2271.4		2267.4	0.269		-0.386	6.597		6.725	6.785		6.904	2268.3	0.394
$^{332}119$	2275.4		2271.8	0.267		-0.415	6.602		6.760	6.793		6.943	2271.4	0.394
$^{333}119$	2279.2		2275.5	0.267		-0.405	6.607		6.755	6.803		6.942	2273.5	0.116
$^{334}119$	2283.0		2279.1	0.268		-0.391	6.613		6.748	6.813		6.938	2276.7	0.117
$^{335}119$	2286.7		2282.9	0.268		-0.383	6.619		6.745	6.823		6.938	2280.7	0.108
$^{336}119$	2290.5		2286.7	0.269		-0.378	6.625		6.747	6.832		6.943	2283.8	0.108
$^{337}119$	2294.1		2290.3	0.269		-0.377	6.630		6.751	6.842		6.950	2288.0	0.108
³³⁸ 119	2297.8		2293.8	0.268		-0.377	6.636		6.757	6.851		6.960	2291.0	0.108
³³⁹ 119	2301.3		2297.1	0.265		-0.378	6.641		6.764	6.860		6.970	2295.0	0.108
³⁴⁰ 119	2304.8		2294.7	0.261		-0.193	6.647		6.613	6.868		6.840		
$^{341}119$	2308.2		2298.0	0.258		-0.188	6.652		6.616	6.876		6.847		
$\frac{342}{343}$ 119	2311.2		2301.2	0.255		-0.185	6.658		6.620	6.885		6.854		
$\frac{343}{344}119$	2314.2		2304.3	0.253		-0.183	6.663		6.625	6.894		6.862		
119	2317.0		2307.4	0.251		-0.180	6.669		6.629	6.904		6.870		

Nuclei BEFRDM β_2 r_t obl. obl. obl. BEprol. sph. obl. prol. sph. prol. sph. prol. sph. β_2 3451192319.8 2310.4 0.249 -0.1786.913 6.674 6.6346.878 $^{346}119$ 2322.62313.3 0.247-0.1766.679 6.6396.9226.886 $^{347}119$ 2325.32316.40.245-0.1746.6836.6436.9316.894 $^{348}119$ 2319.32328.00.243-0.1726.6876.6486.9406.902 $^{349}119$ 2322.22330.70.241-0.1696.6916.6536.9496.910 $^{350}119$ 2333.42325.20.239-0.1666.695 6.6586.958 6.918 $^{351}119$ 2335.9 2328.10.237 -0.1626.699 6.663 6.968 6.926 $^{352}119$ 2338.0 2331.00.234-0.1596.7046.6676.977 6.934 $^{353}119$ 2339.7 2333.9 0.228 -0.1566.7086.6726.9846.942 $^{354}119$ 2341.6 2336.80.221-0.1556.7116.6776.9916.951 $^{355}119$ 2343.42339.70.214-0.1556.7146.6826.998 6.960 $^{356}119$ 2342.52345.30.207 -0.1556.6876.9696.7177.005 $^{357}119$ 2347.22345.20.194 -0.1566.7206.6927.0096.979 $^{358}119$ 2349.2 2347.60.187-0.1816.723 6.7127.016 7.001 $^{359}119$ 2351.12350.10.181-0.1886.7256.7237.0237.015 $^{360}119$ 2352.2-0.1852352.9 0.1766.725 6.7277.0317.023 $^{361}119$ 2354.82354.30.171-0.1796.7266.7297.039 7.030 $^{362}119$ 2356.82356.20.166-0.1736.7286.7307.0487.036 $^{363}119$ 2358.62357.82358.20.1610.091-0.1676.7306.7016.7317.0567.043 $^{364}119$ 2359.92360.36.7322360.30.1530.083-0.1606.7306.7037.0627.028 7.050 $^{365}119$ 2362.42361.8 2362.10.064-0.1546.7296.7056.7337.0667.0347.057 0.143 $^{366}119$ 2363.1 2364.3 2364.50.1620.053 -0.1546.743 6.7387.0897.0427.067 6.708 $^{367}119$ 2364.3 2366.42366.40.1680.047-0.1546.7526.7106.7437.1067.0517.077 $^{368}119$ 2365.72368.52367.97.059 0.1770.036-0.1506.7726.7116.7467.1117.086 $^{369}119$ 2366.22370.52369.30.1950.009 -0.1386.7936.7126.7467.1317.067 7.092 $^{370}119$ 2367.72372.72370.40.2030.002-0.1856.8066.7146.7827.1457.0767.122 $^{371}119$ 2369.12374.70.2062372.00.001-0.2016.8156.7166.8017.1567.0867.140 $^{372}119$ 2370.22376.52373.30.2090.001-0.2076.8246.7186.8117.1687.0967.154 $^{373}119$ 2371.32378.22374.50.2150.001-0.2156.8346.7196.8237.1827.1067.169 $^{374}119$ 2372.4 2379.9 2375.60.224 0.001 -0.2286.842 6.720 6.841 7.1957.116 7.187 $^{375}119$

Table 2. Table 1 is continued....

as such no neutron magic behaviour within this force parameter is exhibited.

2377.0

0.236

0.001

-0.238

6.849

6.721

6.857

7.209

3.3 Shape Coexistence

2373.5

2381.5

The shape of a nucleus is one of the fundamental properties along with its mass and radius. It is the result of the interplay between macroscopic liquid-drop like properties of the nuclear matter and microscopic shell effects. In some areas of the nuclear chart, the shape is seen to be very sensitive to structural effect and may change from one nucleus to its neighbour. These changes are caused by the rearrangement of the orbital configuration of the nucleons or by the dynamic response of the nucleus to rotation. However, there might arise a situation where we may witness that configurations corresponding to different shapes may coexist at similar energies or by a very little difference. The small binding energy difference between two shape configuration makes the structure more complex and the study of such nuclei enrich our understanding of the oscillations of nuclei occurring between two or three existing shapes. This leads isomers can appear in su-

perheavy region. The phenomenon of shape coexistence is ubiquitous as it has been observed throughout the nuclear landscape starting from light nuclei [87] to the regions of heavy nuclei [88,89] and of course in superheavy region [90, 91,92,93,94]. No case of perfect shape-coexistence is observed in considered isotopic chain of Z = 119. However, shape-coexistence can be a common phenomenon in superheavy nuclei and thus it is interesting to study it by future experiments. Here, we noticed a very little energy difference around ≤ 1 MeV in first and second intrinsic excited states in some of the nuclides. For example, in ^{298–318}119 nuclides the excited energy differed by the amount of ≤ 1 MeV within spherical and oblate configurations, whereas prolate suggested to be ground state.

7.126

7.204

3.4 Density profile

In general, the neutron excess becomes larger with increasing the mass number and ofcourse it is quite natural in case of superheavy nuclei providing the largest neutron excesses. However, these nuclei also have large number of protons and therefore huge Coulomb repulsion

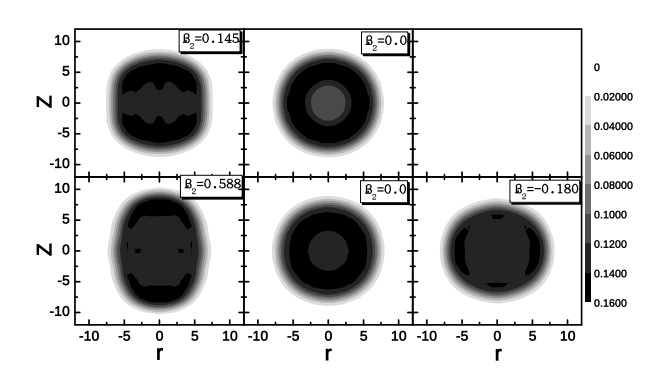


Fig. 4. Two dimensional total matter density contours of ²⁹¹119 and ³⁰³119 for three different shape configurations. Density profile of ²⁹¹119 are seen in upper panel of the figure while the density distribution of ³⁰³119 are represented in lower panel.

exist there that pushes the proton to larger radii and as a result change the proton density distribution. In this view, neutron and proton density distributions are considered to be great source of potential providing fundamental information on nuclear structure and quite useful to identify the special kinds of features of nuclei such as Bubble, Halo/Skin and cluster structures. Such features are observed in light to superheavy nuclei [95,96,97,98, 99,100. In the search of such exotic structures, we have made the plot for total, neutron and proton density profile for predicting neutron shell closure nuclei ²⁹¹119 and ³⁰³119 as shown in Fig. 3. The spherical configuration of these two nuclides show the depletion of central part of neutron, proton and total matter (neutron plus proton) density. At prolate configuration the density dies at r=8fm while it reaches to 10 fm in oblate and spherical configurations. This distribution signals prolate as a ground state of these nuclides. Moreover, spherical structure of these two nuclides indicates a special kind of proton distribution. In which, the centre is little bulgy and a considerably depletion afterward but again a big hump and further distribution tends to zero at the end of the surface following a decreasing pattern. To reveal such anomalous behaviour of nucleon distribution and to visualize the arrangement of nucleons more clearly inside the nuclei, we make two-dimensional contour plots for ²⁹¹119 and ³⁰³119 within three different shape configurations as given in Fig. 4. The full black contour refers to maximum density and full white ones to zero density region. Figure 4 reflects that the hollow region at the centre is spread over the radius of 1-3 fm in spherical configuration. A considerable depopulation is revealed in spherical shape which may supposed to be semi-bubble type structure. It is also apparent that the region from 3-6 fm of total matter density distribution in both the nuclei is highly dense and formed a thick ring type structure. It can be interpreted as a some how hollow central part is surrounded by a thick sheath of nucleons (high density) and formed a thick ring

type structure in prolate shaped. In prolate and oblate configurations, the matter distribution is not uniform and bunches of nucleons far from the centre is seen. These bunches may be the cluster of nucleons or alpha particles. Some spindle type structure is also noticed in prolate configuration having flaps/bulges shapes. In general, cluster, semi-bubble as well as thick ring type structure is seen.

 $\times 10$

3.5 Decay-energies and half-lives

Superheavy nuclei are identified by α —decay followed by spontaneous fission as we have mentioned earlier. Decay energy Q_{α} is the basic parameter to understand the α —decay and used to calculate the half-lives. It is observed in alphaemission and new nucleus is identified. The knowledge of Q_{α} of a nucleus gives a valuable information about its stability. Decay energy is estimated by knowing the binding energies of the parent and daughter nuclei and binding energy of ⁴He nucleus. Here, the binding energies are calculated using the most reliable framework of relativistic mean-field model. Q_{α} is used as a basic input for calculating the α —decay half-life. The quantity Q_{α} is estimated using the relation

$$Q_{\alpha}(N,Z) = BE(N-2,Z-2) + BE(2,2) - BE(N,Z). \tag{15}$$

Here, BE(N, Z), BE(N-2, Z-2), and BE(2, 2) are the binding energies of the parent, daughter and ⁴He (BE = 28.296 MeV [101]) with neutron number N and proton number Z. The values of Q_{α} for ground-state to ground (i.e. prolate) is estimated from RMF binding energy and are given in the Tables 3-6. In order to predict the dominant mode of decay of considered chain, we make the calculations for α -decay, β -decay and spontaneous fission using various empirical formulas and comparison of their life-times shall provide the required results about the mode of decay. The alpha decay half-lives are estimated using various empirical formulas given in literature such as Viola-Seaborg (VSS) [39], Brown [41], Royer [40], generalized liquid drop model (GLDM) [42], Ni et al. [43]. Spontaneous fission half-lives are computed using the semiempirical formula of Ren and Xu [61]. Here, Fiset and Nix [102] empirical formula is used to calculate the β -decay half-lives.

3.5.1 Alpha decay

With the even-even values available at hand, the α -decay half-life of the isotopic chain under study is estimated by Viola-Seaborg semi-empirical relation

$$\log_{10} T_{\frac{1}{2}}^{\alpha} = \frac{aZ - b}{\sqrt{Q_{\alpha}}} - (cZ + d) + h_{\log}.$$
 (16)

The values of the parameters a, b, c and d are taken from the recent modified parameterizations of Sobiczewski et al [47], which are a = 1.66175, b = 8.5166, c = 0.20,

Table 3. Decay energies (in MeV) and half-lives of α , β and spontaneous fission (in seconds) for Z=119 isotopic chain and prediction of mode of decays is given.

Nuclei	Q_{α}^{RMF}	Q_{α}^{FRDM}			los	$g(T_{1/2}^{\alpha})$			$\log(T_{1/2}^{SF})$	Q_{β}^{RMF}	Q_{β}^{FRDM}	$\log(T_{1/2}^{\beta})$	$T_{1/2}^{\beta}$	Mode of
1.40101	α	Ψα	VSS	Brown			Ni et. al.			₹ Þ	₹ β	Fiset-Nix		
284119	14.00	13.02	-6.29	-6.98	-6.86	-6.64	-7.29	-4.42	1.17	14.29	10.35	0.03	3.73	α
	13.89	13.79	-6.43	-6.79	-6.67	-6.81	-7.66	-6.25	5.73	14.41	8.80	0.05	3.63	α
$^{286}_{237}119$	13.83	13.74	-5.97	-6.69	-6.57	-6.33	-7.00	-5.81	9.45	14.47	9.69	0.03	5.75	α
	13.79	13.45	-6.26	-6.63	-6.53	-6.67	-7.51	-5.60	12.34	14.50	7.97	0.05	4.45	α
	13.99	13.38	-6.27	-6.95	-6.90	-6.69	-7.26	-5.14	14.40	14.30	8.87	0.03	5.82	α
$^{289}_{290}119$	14.12	13.35	-6.84	-7.15	-7.15	-7.30	-8.01	-5.79	15.65	7.92	7.55	0.22	12.84	α
$^{291}119$	14.22	13.36 13.20	-6.68 -7.30	-7.31 -7.56	-7.35 -7.64	-7.16 -7.80	-7.61 -8.40	-5.09 -5.13	$16.09 \\ 15.74$	$7.67 \\ 7.43$	$8.21 \\ 6.76$	$0.06 \\ 0.38$	21.97 41.09	α
$^{292}119$	14.30	13.20 13.17	-7.08	-7.66	-7.78	-7.62	-8.40 -7.95	-3.13 -4.71	13.74 14.59	6.53	7.71	0.38 0.45	27.00	α
	15.32	12.88	-8.86	-8.92	-9.22	-7.02 -9.39	-7.93 -9.73	-4.71 -4.47	12.67	6.30	6.03	0.43 0.78	73.84	lpha
004	15.13	12.80	-8.22	-8.66	-8.95	-8.87	-8.93	-3.97	9.97	5.98	6.85	0.66	80.88	α
$^{295}119$	16.18	12.88	-10.16		-10.56		-10.85	-4.49	6.51	4.81	5.45	1.42	>100	α
$^{296}119$	16.02	13.08	-9.58	-9.86	-10.34	-10.36	-10.10	-4.54	2.29	5.41	6.77	0.91	28.29	α
	16.03	12.74	-9.95	-9.88	-10.38	-10.56	-10.67	-4.19	-2.69	5.10	5.19	1.29	71.00	α
	11.48	12.50	-1.01	-2.33	-1.84	-1.25	-2.76	-3.34	-8.40	5.01	5.68	1.09	>100	SF
$^{299}119$	11.37	12.80	-1.09	-2.10	-1.60	-1.72	-3.09	-4.32	-14.85	3.38	4.18	2.25	> 100	SF
$^{300}119$	9.96	13.15	3.11	1.28	2.22	3.11	0.76	-4.67	-22.03	9.70	4.92	-0.51	> 100	SF
$^{301}_{202}119$	11.04	13.27	-0.25	-1.30	-0.80	-0.92	-2.37	-5.25	-29.93	4.38	3.55	1.66	> 100	$_{ m SF}$
$\frac{302}{202}$ 119	11.09	13.38	-0.04	-1.48	-0.95	-0.29	-1.93	-5.13	-38.54	4.07	4.34	1.58	>100	$_{\rm SF}$
³⁰³ 119	11.24	13.38	-0.76	-1.82	-1.34	-1.47	-2.81	-5.46	-47.86	3.72	2.16	2.04	>100	$_{ m SF}$
$\frac{304}{305110}$	11.65	14.14	-1.42	-2.70	-2.36	-1.79	-3.11	-6.55	-57.88	3.27	3.99	2.09	>100	$_{ m SF}$
$^{305}119$ $^{306}119$	11.95	13.84	-2.47	-3.31	-3.07	-3.21	-4.27	-6.33	-68.59	2.83	1.59	2.66	>100	$_{ m SF}$
307119	6.44	13.97	17.69	14.09	16.65	18.57	13.25	-6.23	-79.98	8.25	3.28	-0.10	>100	$_{ m SF}$
308 ₁₁₉	5.88	13.81	20.81	17.12	20.07	20.06	15.65	-6.29	-92.06	8.43	1.27	0.09	>100	$_{ m SF}$
$^{309}119$	5.31 9.03	13.43 13.31	25.26 5.76	20.73 3.91	24.14 5.05	$26.61 \\ 4.95$	$19.72 \\ 2.77$	-5.23 -3.35	-104.80 -118.22	$1.61 \\ 1.36$	$\frac{2.64}{0.96}$	$\frac{3.60}{4.18}$	>100 >100	SF
$^{310}119$	9.03 8.88	12.76	6.63	$\frac{3.91}{4.38}$	5.57	6.70	$\frac{2.77}{3.78}$	-3.33 -3.88	-110.22	1.08	1.99	4.16 4.35	>100	SF
$^{311}119$	8.91	12.49	6.21	4.30	5.46	5.37	3.16	-3.65	-132.23	0.81	0.51	5.08	>100	SF
$^{312}119$	6.81	12.11	15.63	12.27	14.49	16.27	11.48	-2.48	-162.39	1.02	±	4.46	±	SF
$^{313}119$	6.30	13.25	18.17	14.80	17.34	17.31	13.40	-5.22	-178.39	0.69	6.28	5.33	14.29	SF
$^{314}119$	8.28	4.66	8.91	6.37	7.76	9.06	5.73	>20	-195.05	-3.42	1.30	2.00	>100	SF
$^{315}119$	9.34	4.13	4.70	2.98	3.89	3.79	1.87	>20	-212.32	-4.74	\pm	1.49	stable	SF
$^{316}119$	9.17	5.14	5.64	3.50	4.47	5.54	2.93	>20	-230.22	0.45	1.27	5.70	>100	SF
$^{317}119$	9.25	8.14	5.01	3.25	4.17	4.07	2.14	9.11	-248.73	0.41	3.77	6.04	1.14	SF
$^{318}119$	9.33	7.84	5.08	3.01	3.88	4.91	2.45	10.74	-267.86	0.05	\pm	7.47	\pm	SF
$^{319}119$	9.40	8.74	4.51	2.81	3.64	3.54	1.71	6.79	-287.59	-0.12	0.57	7.18	> 100	SF
$^{320}119$	9.07	8.68	5.97	3.80	4.74	5.83	3.22	7.36	-307.92	-0.15	2.05	6.77	> 100	SF
$^{321}_{222}119$	8.71	8.71	6.91	4.92	5.99	5.90	3.76	6.92	-328.84	-0.34	1.19	6.27	> 100	SF
$\frac{322}{323}$ 119	8.42	8.72	8.36	5.90	7.09	8.35	5.26	7.21	-350.35	-0.50	2.69	5.56	>100	$_{ m SF}$
$\frac{323}{324}$ 119	8.17	8.98	9.01	6.76	8.05	7.97	5.56	5.94	-372.45	-0.53	1.89	5.72	>100	$_{ m SF}$
$^{324}_{325}119$	8.01	9.00	10.00	7.33	8.69	10.06	6.67	6.21	-395.12	-0.70	3.36	5.09	71.06	$_{ m SF}$
$^{326}119$	7.80	8.94	10.57	8.13	9.57	9.50	6.89	6.09	-418.36	-0.88	$\frac{2.41}{2.72}$	4.96	>100	SF
$^{327}119$	$7.87 \\ 7.82$	$8.72 \\ 8.55$	10.61 10.48	$7.87 \\ 8.05$	$9.26 \\ 9.45$	$10.68 \\ 9.38$	$7.18 \\ 6.82$	$7.21 \\ 7.52$	-442.17 -466.54	-1.12 -1.33	$3.73 \\ 2.82$	$4.31 \\ 4.24$	22.28 17.84	$_{ m SF}$
$^{328}119$	7.82	8.27	10.48	8.11	9.40	10.94	7.42	8.95	-400.54 -491.47	-1.33 -1.47	$\frac{2.82}{4.08}$	3.81	31.41	SF
$^{329}119$	7.72	8.08	10.88	8.43	9.85	9.77	7.42	9.35	-516.95	-1.47	3.16	3.93	54.58	SF
$^{330}119$	7.53	6.24	12.11	9.19	10.69	12.22	8.47	18.92	-542.98	-1.66	$\frac{3.10}{2.57}$	3.57	>100	SF
$^{331}119$	7.49	6.03	11.92	9.32	10.82	10.75	8.05	19.87	-569.54	-1.80	1.65	3.66	>100	SF
$^{332}119$	7.45	5.98	12.48	9.51	11.02	12.58	8.79	>20	-596.65	-2.01	2.96	3.19	>100	SF
$^{333}119$	7.44	7.82	12.16	9.53	11.03	10.96	8.26	10.48	-624.28	-2.22	5.96	3.22	0.08	SF
$^{334}119$	7.33	7.57	13.05	10.01	11.56	13.15	9.27	11.9	-652.44	-2.41	4.85	2.80	>100	SF
$^{335}119$	7.17	7.42	13.46	10.67	12.29	12.23	9.37	12.28	-681.13	-2.60	3.61	2.88	>100	SF
$^{336}119$	6.91	7.16	15.12	11.83	13.59	15.33	11.05	13.86	-710.33	-2.79	5.02	2.49	4.52	SF
$^{337}119$	6.72	6.76	15.78	12.70	14.57	14.51	11.35	15.58	-740.04	-2.97	3.86	2.60	43.33	SF
³³⁸ 119	6.53	6.54	17.17	13.62	15.59	17.48	12.80	17.11	-770.27	-3.15	5.33	2.22	9.55	SF
$^{339}119$	6.39	6.36	17.63	14.33	16.38	16.34	12.94	17.82	-800.99	-3.38	4.32	2.30		SF
$^{340}119$	6.32		18.44	14.74	16.83	18.81	13.89		-832.22	-3.65		1.89		$_{\rm SF}$
$\frac{341}{342}$ 119	6.12		19.29	15.79	18.00	17.96	14.35		-863.94	-3.99		1.93		$_{ m SF}$
$\frac{342}{343110}$	6.09		19.81	15.95	18.17	20.24	15.06		-896.15	-4.46		1.43		$_{ m SF}$
$\frac{343}{344}$ 119	6.00		20.05	16.46	18.73	18.70	15.01		-928.85	-4.80		1.50		$_{ m SF}$
³⁴⁴ 119	5.89		21.08	17.06	19.40	21.57	16.15		-962.03	-5.03		1.15		SF

Nuclei	$Q_{\alpha}^{RMF} Q_{\alpha}^{FRDM}$	ſ		lo	$g(T_{1/2}^{\alpha})$		$\log(T_{1/2}^{SF})$	Q_{β}^{RMF}	Q_{β}^{FRDM}	$\log(T_{1/2}^{\beta})$	$T_{1/2}^{\beta}$	Mode of
			Brown	Royer	GLDM	Ni et. al.	FRDM Ren-Xu			Fiset-Nix		decay
345119	5.61	22.72	18.80	21.36	21.34	17.30	-995.69	-5.25		1.29		SF
$^{346}119$	5.30	25.32	20.79	23.60	26.07	19.78	-1029.82	-5.49		0.95		SF
$^{347}119$	5.16	26.12	21.79	24.71	24.71	20.20	-1064.42	-5.68		1.11		SF
$^{348}119$	4.90	28.66	23.71	26.88	29.59	22.63	-1099.49	-5.82		0.81		SF
$^{349}119$	4.67	30.35	25.50	28.89	28.91	23.82	-1135.01	-5.93		1.01		SF
$^{350}119$	4.48	32.58	27.16	30.76	33.75	25.99	-1170.99	-6.05		0.72		SF
$^{351}119$	4.49	32.13	27.06	30.63	30.66	25.34	-1207.44	-6.29		0.87		SF
$^{352}119$	5.00	27.78	22.94	25.95	28.59	21.88	-1244.33	-6.88		0.41		SF
$^{353}119$	5.65	22.40	18.52	20.91	20.89	17.02	-1281.67	-7.24		0.53		SF
$^{354}119$	5.69	22.46	18.27	20.62	22.88	17.33	-1319.44	-7.32		0.27		SF
$^{355}119$	5.56	23.07	19.11	21.56	21.53	17.60	-1357.66	-7.37		0.49		SF
$^{356}119$	5.38	24.70	20.24	22.82	25.25	19.25	-1396.31	-7.45		0.23		SF
$^{357}119$	5.19	25.84	21.54	24.28	24.27	19.96	-1435.39	-7.43		0.48		SF
$^{358}119$	5.05	27.36	22.57	25.44	28.05	21.52	-1474.91	-7.48		0.22		SF
$^{359}119$	4.86	28.67	24.02	27.07	27.07	22.38	-1514.84	-7.60		0.42		SF
$^{360}119$	4.91	28.58	23.64	26.62	29.32	22.57	-1555.19	-7.69		0.15		SF
$^{361}119$	4.86	28.60	23.96	26.96	26.97	22.32	-1595.97	-7.71		0.39		SF
$^{362}119$	4.67	30.69	25.50	28.70	31.55	24.37	-1637.15	-7.73		0.14		SF
$^{363}119$	4.61	30.97	26.04	29.30	29.31	24.35	-1678.74	-7.83		0.36		SF
$^{364}119$	4.80	29.47	24.43	27.45	30.22	23.33	-1720.75	-10.22		-0.54		SF
$^{365}119$	4.97	27.65	23.13	25.96	25.96	21.51	-1763.16	-8.13		0.27		SF
³⁶⁶ 119	4.11	36.49		34.41	37.68	29.34	-1805.96			0.72		SF
$^{367}119$	3.55	43.17	36.76	41.39	41.47	34.80	-1849.16	-5.67		1.14		SF
$^{368}119$	6.37		14.45	16.07	18.03	13.60	-1892.76			-0.24		SF
$^{369}119$	6.63	16.30	13.16	14.60	14.53	11.79	-1936.75	-9.16		-0.02		SF
$^{370}119$	7.02	14.58		12.53	14.24	10.59	-1981.12	-9.28		-0.29		SF
$^{371}_{272}119$	3.48	44.22		42.38	42.46	35.69	-2025.88			-0.08		SF
$^{372}119$	3.39	45.85		43.65	47.58	37.35	-2071.02			-0.39		SF
$^{373}119$	3.27		40.52	45.57	45.67	38.46	-2116.53			-0.21		SF
$^{374}119$	3.07		43.39	48.81	53.12	41.81	-2162.42			-0.51		SF
$^{375}119$	2.99	52.30	44.77	50.37	50.49	42.61	-2208.69	-10.18		-0.27		$_{ m SF}$

Table 4. Table 3 is continued.....

d=33.9069. The h_{\log} is the hindrance factor which takes the care of odd numbers of proton and neutron as given by Viola and Seaborg

$$h_{\log} = \begin{cases} 0.000 \ even - even; \\ 0.772 \ odd - even; \\ 1.066 \ even - odd; \\ 1.114 \ odd - odd. \end{cases}$$
 (17)

There are also several other phenomenological formulas available in the literature by which the α -decay half-lives is calculated. The semi-empirical formula proposed by Brown [41] for determining the half-life of superheavy nuclei is given by

$$\log_{10} T_{\frac{1}{2}}^{\alpha} = 9.54(Z-2)^{0.6} / \sqrt{Q_{\alpha}} - 51.37, \qquad (18)$$

where Z, the atomic number of parent nucleus and Q_{α} decay energy are only the input for this formula. Moreover, another theoretical predictions for half-life for heavy and superheavy nuclei by employing a fitting procedure to a set of 373 alpha emitters was developed by Royer [40] with

an RMS deviation of 0.42, given as

$$\log_{10} T_{1/2}^{\alpha} = -26.06 - 1.114 A^{1/6} \sqrt{Z} + \frac{1.5837 Z}{\sqrt{Q_{\alpha}}}, \quad (19)$$

where A and Z represent the mass number and charge number of the parent nuclei and Q_{α} represents the energy released during the reaction. Assuming a similar dependence on A, Z and Q_{α} , the above equation was reformulated for a subset of 131 even-even nuclei and a relation was obtained with a RMS deviation of only 0.285, given,

$$\log_{10} T_{1/2}^{\alpha} = -25.31 - 1.1629 A^{1/6} \sqrt{Z} + \frac{1.5864Z}{\sqrt{Q_{\alpha}}}.$$
 (20)

For a subset of 106 even-odd nuclei, the relation given by was further modified with an RMS deviation of 0.39, and is given as,

$$\log_{10} T_{1/2}^{\alpha} = -26.65 - 1.0859 A^{1/6} \sqrt{Z} + \frac{1.5848Z}{\sqrt{Q_{\alpha}}}.$$
 (21)

A similar reformulation was performed for the equation for a subset of 86 odd-even nuclei and 50 odd-odd nuclei.

Table 5. Possible α -decay chains of fission survival nuclides i.e. $^{284-297}119$ of the considered isotopic chain. Experimental data for Q_{α} [104,105,106], if available, is given in parentheses with asterisk.

	ORME			TRO ()			mSF()	3.f. 1. C
Nuclei	Q_{lpha}^{RMF}	- VOC	D	$T_{1/2}^{\alpha}(\mathrm{sec})$	CLDM	NT: 4 1	$T_{1/2}^{SF}(\mathrm{sec})$	Mode of
²⁸⁴ 119	14.00	$\frac{\text{VSS}}{0.502 \times 10^{-06}}$	$\frac{\text{Brown}}{0.106 \times 10^{-06}}$	$\frac{\text{Royer}}{0.139 \times 10^{-06}}$	$\frac{\text{GLDM}}{0.227 \times 10^{-06}}$	Ni et. al. 0.518×10^{-07}	Ren-Xu $0.149 \times 10^{+02}$	decay
$^{280}{\rm Ts}$	14.005	0.502×10^{-05} 0.398×10^{-05}	0.106×10^{-06} 0.615×10^{-06}	0.139×10^{-05} 0.102×10^{-05}	0.227×10^{-05} 0.183×10^{-05}	0.518×10^{-06} 0.286×10^{-06}	0.149×10^{-03} 0.470×10^{-03}	$\alpha 1$
$^{276}\mathrm{Mc}$	13.257		0.836×10^{-05}	0.102×10^{-04} 0.189×10^{-04}	0.183×10^{-04} 0.392×10^{-04}	0.286×10^{-05} 0.347×10^{-05}	0.470×10^{-06}	$\alpha 2$
	12.353	0.783×10^{-04}					0.358×10^{-06}	SF
²⁷² Nh	12.032	0.107×10^{-03}	0.109×10^{-04}	0.245×10^{-04}	0.490×10^{-04}	0.432×10^{-05}	0.553×10^{-08}	$_{ m SF}$
$^{268}\mathrm{Rg}$	11.714	0.144×10^{-03}	0.142×10^{-04}	0.317×10^{-04}	0.611×10^{-04}	0.536×10^{-05}	0.145×10^{-08}	SF
$^{285}119$	13.891	0.368×10^{-06}	0.160×10^{-06}	0.214×10^{-06}	0.153×10^{-06}	0.219×10^{-07}	$0.539 \times 10^{+06}$	$\alpha 1$
$^{281}\mathrm{Ts}$	13.396	0.982×10^{-06}	0.358×10^{-06}	0.533×10^{-06}	0.388×10^{-06}	0.475×10^{-07}	$0.948 \times 10^{+01}$	α^2
$^{277}\mathrm{Mc}$	12.286	0.494×10^{-04}	0.112×10^{-04}	0.250×10^{-04}	0.189×10^{-04}	0.129×10^{-05}	0.340×10^{-02} 0.390×10^{-02}	$\alpha 3$
$^{273}\mathrm{Nh}$	11.873	0.108×10^{-03}	0.222×10^{-04}	0.519×10^{-04}	0.399×10^{-04}	0.129×10^{-05} 0.240×10^{-05}	0.317×10^{-04}	$\alpha 4/SF$
269 Rg	11.398	0.335×10^{-03}	0.222×10^{-04} 0.619×10^{-04}	0.313×10^{-03} 0.155×10^{-03}	0.122×10^{-03}	0.609×10^{-05}	0.424×10^{-05}	SF
ng	11.990	0.555 × 10	0.019 × 10	0.100 × 10	0.122 × 10	0.009 × 10	0.424 \(10	ŊI.
$^{286}119$	13.827	0.106×10^{-05}	0.203×10^{-06}	0.269×10^{-06}	0.464×10^{-06}	0.981×10^{-07}	$0.282 \times 10^{+10}$	$\alpha 1$
$^{282}\mathrm{Ts}$	13.296	0.335×10^{-05}	0.528×10^{-06}	0.792×10^{-06}	0.140×10^{-05}	0.246×10^{-06}	$0.309 \times 10^{+05}$	$\alpha 2$
$^{278}\mathrm{Mc}$	12.306	0.984×10^{-04}	0.103×10^{-04}	0.218×10^{-04}	0.460×10^{-04}	0.422×10^{-05}	$0.779 \times 10^{+01}$	$\alpha 3$
$^{274}\mathrm{Nh}$	11.668	0.674×10^{-03}	0.568×10^{-04}	0.142×10^{-03}	0.323×10^{-03}	0.209×10^{-04}	0.377×10^{-01}	$\alpha 4$
$^{270}\mathrm{Rg}$	11.262	0.152×10^{-02}	0.119×10^{-03}	0.305×10^{-03}	0.695×10^{-03}	0.403×10^{-04}	0.292×10^{-02}	$\alpha 5$
$^{266}\mathrm{Mt}$	10.160	$0.205 \times 10^{+00}$	0.107×10^{-01}	0.399×10^{-01}	$0.122 \times 10^{+00}$	0.264×10^{-02}	0.299×10^{-02}	SF
$^{262}\mathrm{Bh}$	10.215	0.339×10^{-01}	0.220×10^{-02}	0.646×10^{-02}	0.163×10^{-01}	0.551×10^{-03}	0.329×10^{-01}	SF
207		0.0	0.0	0.0	0.0	0.7	. 10	
$^{287}119$	13.795	0.553×10^{-06}	0.229×10^{-06}	0.295×10^{-06}	0.210×10^{-06}	0.310×10^{-07}	$0.217 \times 10^{+13}$	$\alpha 1$
$^{283}{ m Ts}$	13.092	0.379×10^{-05}	0.118×10^{-05}	0.188×10^{-05}	0.138×10^{-05}	0.151×10^{-06}	$0.168 \times 10^{+08}$	$\alpha 2$
$^{279}\mathrm{Mc}$	12.296	0.470×10^{-04}	0.107×10^{-04}	0.219×10^{-04}	0.165×10^{-04}	0.124×10^{-05}	$0.289 \times 10^{+04}$	$\alpha 3$
$^{275}\mathrm{Nh}$	11.629	0.376×10^{-03}	0.681×10^{-04}	0.167×10^{-03}	0.128×10^{-03}	0.699×10^{-05}	$0.942 \times 10^{+01}$	$\alpha 4$
271 Rg	11.077	0.188×10^{-02}	0.295×10^{-03}	0.797×10^{-03}	0.631×10^{-03}	0.268×10^{-04}	$0.480 \times 10^{+00}$	$\alpha 5$
$^{267}\mathrm{Mt}$	9.963	$0.319 \times 10^{+00}$	0.329×10^{-01}	$0.131 \times 10^{+00}$	$0.108 \times 10^{+00}$	0.213×10^{-02}	$0.317 \times 10^{+00}$	$\alpha 6$
$^{263}\mathrm{Bh}$	10.086	0.336×10^{-01}	0.450×10^{-02}	0.135×10^{-01}	0.112×10^{-01}	0.302×10^{-03}	$0.219 \times 10^{+01}$	$\alpha 7$
²⁸⁸ 119	13.939	0.537×10^{-06}	0.112×10^{-06}	0.126×10^{-06}	0.207×10^{-06}	0.548×10^{-07}	$0.252 \times 10^{+15}$	$\alpha 1$
$^{284}\mathrm{Ts}$	12.970	0.145×10^{-04}	0.112×10^{-05} 0.193×10^{-05}	0.314×10^{-05}	0.615×10^{-05}	0.865×10^{-06}	0.252×10^{-10} $0.153 \times 10^{+10}$	$\alpha 1$
$^{280}\mathrm{Mc}$	12.042	0.363×10^{-03}	0.328×10^{-04}	0.737×10^{-04}	0.013×10^{-03} 0.171×10^{-03}	0.129×10^{-04}	$0.204 \times 10^{+06}$	$\alpha 2$
^{276}Nh	11.541	0.303×10^{-02} 0.131×10^{-02}	0.103×10^{-03}	0.757×10^{-03} 0.252×10^{-03}	0.604×10^{-03}	0.370×10^{-04}	$0.505 \times 10^{+03}$	$\alpha 4$
272 Rg	10.971	0.744×10^{-02}	0.502×10^{-03}	$0.232 \times 10^{-0.02}$ $0.137 \times 10^{-0.02}$	0.351×10^{-02}	0.370×10^{-03} 0.158×10^{-03}	$0.192 \times 10^{+02}$	α 5
$^{268}\mathrm{Mt}$	10.409	0.744×10 0.458×10^{-01}	$0.302 \times 10^{-0.02}$ $0.273 \times 10^{-0.02}$	0.137×10^{-02} 0.819×10^{-02}	0.331×10^{-01} 0.224×10^{-01}	0.728×10^{-03}	$0.192 \times 10^{-0.1}$ $0.928 \times 10^{+0.1}$	$\alpha 6$
^{264}Bh	9.358	$0.498 \times 10^{-0.408} \times 10^{-0$	$0.273 \times 10^{+00}$ $0.335 \times 10^{+00}$	$0.819 \times 10^{-0.141} \times 10^{+0.11}$	$0.524 \times 10^{-0.526} \times 10^{+0.526}$	0.600×10^{-01}	$0.463 \times 10^{+02}$	$\frac{\alpha \sigma}{\alpha 7}$
$^{260}\mathrm{Db}$	9.556 8.543	$0.563 \times 10^{+03}$	$0.353 \times 10^{+02}$ $0.193 \times 10^{+02}$	$0.141 \times 10^{-0.00}$ $0.986 \times 10^{+0.00}$	$0.326 \times 10^{+03}$ $0.472 \times 10^{+03}$	$0.000 \times 10^{-0.00} \times 10^{-0.00}$	$0.403 \times 10^{-0.4}$ $0.191 \times 10^{+0.4}$	
$^{256}\mathrm{Lr}$		$0.363 \times 10^{+06}$ $0.105 \times 10^{+06}$	$0.193 \times 10^{+04}$ $0.302 \times 10^{+04}$	$0.986 \times 10^{+05}$ $0.188 \times 10^{+05}$	$0.472 \times 10^{+06}$ $0.123 \times 10^{+06}$	$0.229 \times 10^{+03}$ $0.206 \times 10^{+03}$	$0.191 \times 10^{+06}$ $0.522 \times 10^{+06}$	α8 - 0/CE
Lľ	7.690	0.105 × 10	0.302 × 10	0.188 × 10	0.123 × 10	0.200 × 10	0.522 × 10	$\alpha 9/\mathrm{SF}$
$^{289}119$	14.116	0.145×10^{-06}	0.706×10^{-07}	0.714×10^{-07}	0.504×10^{-07}	0.982×10^{-08}	$0.447 \times 10^{+16}$	$\alpha 1$
$^{285}\mathrm{Ts}$	13.015	0.537×10^{-05}	0.161×10^{-05}	0.246×10^{-05}	0.179×10^{-05}	0.205×10^{-06}	$0.239 \times 10^{+11}$	$\alpha 2$
$^{281}\mathrm{Mc}$	11.770	0.665×10^{-03}	0.114×10^{-03}	0.283×10^{-03}	0.216×10^{-03}	0.119×10^{-04}	$0.278 \times 10^{+07}$	$\alpha 3$
$^{277}\mathrm{Nh}$	11.462	0.904×10^{-03}	0.149×10^{-03}	0.367×10^{-03}	0.284×10^{-03}	0.149×10^{-04}	$0.589 \times 10^{+04}$	$\alpha 4$
$^{273}\mathrm{Rg}$	10.931	0.423×10^{-02}	0.615×10^{-03}	0.165×10^{-02}	0.131×10^{-02}	0.537×10^{-04}	$0.189 \times 10^{+03}$	$\alpha 5$
$^{269}{ m Mt}$	10.211	0.684×10^{-01}	0.807×10^{-02}	0.258×10^{-01}	0.211×10^{-01}	0.567×10^{-03}	$0.762 \times 10^{+02}$	$\alpha 6$
$^{265}\mathrm{Bh}$	9.216	$0.969 \times 10^{+01}$	$0.822 \times 10^{+00}$	$0.359 \times 10^{+01}$	$0.306 \times 10^{+01}$	0.390×10^{-01}	$0.312 \times 10^{+03}$	$\alpha 7$
$^{261}\mathrm{Db}$	8.316	$0.151 \times 10^{+04}$	$0.999 \times 10^{+02}$	$0.558 \times 10^{+03}$	$0.497 \times 10^{+03}$	$0.295 \times 10^{+01}$	$0.104 \times 10^{+05}$	$\alpha 8$
$^{257}\mathrm{Lr}$	7.597	$0.109 \times 10^{+06}$	$0.653 \times 10^{+04}$	$0.412 \times 10^{+05}$	$0.380 \times 10^{+05}$	$0.118 \times 10^{+03}$	$0.227 \times 10^{+07}$	$\alpha 9$
200		0.000 06	0.40- :- 07		0.000 07	0.044 07	0.404 :-117	_
²⁹⁰ 119	14.219	0.208×10^{-06}	0.487×10^{-07}	0.451×10^{-07}	0.693×10^{-07}	0.244×10^{-07}	$0.124 \times 10^{+17}$	$\alpha 1$
$^{286}{ m Ts}$	13.114	0.754×10^{-05}	0.108×10^{-05}	0.151×10^{-05}	0.281×10^{-05}	0.494×10^{-06}	$0.657 \times 10^{+11}$	$\alpha 2$
$^{282}{ m Mc}$	11.617	0.327×10^{-02}	0.232×10^{-03}	0.606×10^{-03}	0.165×10^{-02}	0.848×10^{-04}	$0.745 \times 10^{+07}$	$\alpha 3$
^{278}Nh	$11.057 (11.60)^*$	0.182×10^{-01}	0.109×10^{-02}	0.321×10^{-02}	0.926×10^{-02}	0.352×10^{-03}	$0.152 \times 10^{+05}$	$\alpha 4$
274 Rg	$10.975 (11.15)^*$	0.727×10^{-02}	0.492×10^{-03}	0.124×10^{-02}	0.315×10^{-02}	0.155×10^{-03}	$0.469 \times 10^{+03}$	$\alpha 5$
$^{270}{ m Mt}$	$10.282 (10.03)^*$	0.978×10^{-01}	0.545×10^{-02}	0.161×10^{-01}	0.465×10^{-01}	0.140×10^{-02}	$0.178 \times 10^{+03}$	$\alpha 6$
$^{266}\mathrm{Bh}$	8.901	$0.202 \times 10^{+03}$	$0.653 \times 10^{+01}$	$0.328 \times 10^{+02}$	$0.154 \times 10^{+03}$	$0.961 \times 10^{+00}$	$0.681 \times 10^{+03}$	$\alpha 7/\mathrm{SF}$
$^{262}\mathrm{Db}$	8.132	$0.147 \times 10^{+05}$	$0.398 \times 10^{+03}$	$0.238 \times 10^{+04}$	$0.144 \times 10^{+05}$	$0.378 \times 10^{+02}$	$0.211 \times 10^{+05}$	$\alpha 8/\mathrm{SF}$
258 Lr	7.446	$0.947 \times 10^{+06}$	$0.235 \times 10^{+05}$	$0.156 \times 10^{+06}$	$0.120 \times 10^{+07}$	$0.136 \times 10^{+04}$	$0.421 \times 10^{+07}$	$\alpha 9/\mathrm{SF}$

Table 6. Table 5 is continued.....

Nuclei	Q_{α}^{RMF}			$T_{1/2}^{\alpha}(\mathrm{sec})$			$T_{1/2}^{SF}(\mathrm{sec})$	Mode of
	• α	VSS	Brown	Royer	GLDM	Ni et. al.	Ren-Xu	decay
$^{291}119$	14.378	0.499×10^{-07}	0.278×10^{-07}	0.228×10^{-07}	0.160×10^{-07}	0.396×10^{-08}	$0.548 \times 10^{+16}$	$\alpha 1$
$^{287}\mathrm{Ts}$	13.071	0.417×10^{-05}	0.129×10^{-05}	0.175×10^{-05}	0.128×10^{-05}	0.164×10^{-06}	$0.321 \times 10^{+11}$	$\alpha 2$
$^{283}\mathrm{Mc}$	11.570	0.419×10^{-02}	0.291×10^{-03}	0.778×10^{-03}	0.215×10^{-02}	0.105×10^{-03}	$0.399 \times 10^{+07}$	$\alpha 3$
$^{279}\mathrm{Nh}$	10.712	$0.132 \times 10^{+00}$	0.649×10^{-02}	0.232×10^{-01}	0.773×10^{-01}	0.193×10^{-02}	$0.888 \times 10^{+04}$	$\alpha 4$
275 Rg	10.962	0.782×10^{-02}	0.525×10^{-03}	0.133×10^{-02}	0.340×10^{-02}	0.165×10^{-03}	$0.294 \times 10^{+03}$	$\alpha 5$
$^{271}\mathrm{Mt}$	10.320	0.354×10^{-01}	0.443×10^{-02}	0.123×10^{-01}	0.997×10^{-02}	0.322×10^{-03}	$0.119 \times 10^{+03}$	$\alpha 6$
$^{267}\mathrm{Bh}$	8.729	$0.332 \times 10^{+03}$	$0.212 \times 10^{+02}$	$0.113 \times 10^{+03}$	$0.981 \times 10^{+02}$	$0.811 \times 10^{+00}$	$0.489 \times 10^{+03}$	$\alpha 7/\mathrm{SF}$
$^{263}\mathrm{Db}$	7.786	$0.127 \times 10^{+06}$	$0.611 \times 10^{+04}$	$0.437 \times 10^{+05}$	$0.397 \times 10^{+05}$	$0.133 \times 10^{+03}$	$0.161 \times 10^{+05}$	$\alpha 8/\mathrm{SF}$
$^{259}\mathrm{Lr}$	7.334	$0.122 \times 10^{+07}$	$0.625 \times 10^{+05}$	$0.426 \times 10^{+06}$	$0.398 \times 10^{+06}$	$0.937 \times 10^{+03}$	$0.337 \times 10^{+07}$	$\alpha 9/\mathrm{SF}$
202		07		07	07	07		
$^{292}_{288}$ 119	14.450	0.828×10^{-07}	0.217×10^{-07}	0.165×10^{-07}	0.238×10^{-07}	0.111×10^{-07}	$0.394 \times 10^{+15}$	$\alpha 1$
$^{288}{ m Ts}$	13.081	0.875×10^{-05}	0.124×10^{-05}	0.161×10^{-05}	0.304×10^{-05}	0.561×10^{-06}	$0.284 \times 10^{+10}$	$\alpha 2$
$^{284}{ m Mc}$	11.552	0.462×10^{-02}	0.317×10^{-03}	0.788×10^{-03}	0.219×10^{-02}	0.114×10^{-03}	$0.434 \times 10^{+06}$	$\alpha 3$
280 Nh	10.486	0.510×10^{-00}	0.218×10^{-01}	0.823×10^{-01}	0.302×10^{-00}	0.614×10^{-02}	$0.118 \times 10^{+04}$	$\alpha 4$
276 Rg	10.434	0.166×10^{-00}	0.836×10^{-02}	0.259×10^{-01}	0.827×10^{-01}	0.227×10^{-02}	$0.478 \times 10^{+02}$	$\alpha 5$
$^{272}{ m Mt}$	10.560	0.189×10^{-01}	0.122×10^{-02}	0.286×10^{-02}	0.736×10^{-02}	0.341×10^{-03}	$0.236 \times 10^{+02}$	$\alpha 6$
268 Bh	8.804	$0.415 \times 10^{+03}$	$0.126 \times 10^{+02}$	$0.618 \times 10^{+02}$	$0.307 \times 10^{+03}$	$0.178 \times 10^{+01}$	$0.117 \times 10^{+03}$	$\alpha 7/\mathrm{SF}$
264 Db	7.442	$0.640 \times 10^{+07}$	$0.111 \times 10^{+06}$	$0.964 \times 10^{+06}$	$0.901 \times 10^{+07}$	$0.699 \times 10^{+04}$	$0.463 \times 10^{+04}$	SF
$^{260}\mathrm{Lr}$	7.144	$0.167 \times 10^{+08}$	$0.345 \times 10^{+06}$	$0.255 \times 10^{+07}$	$0.241 \times 10^{+08}$	$0.160 \times 10^{+05}$	$0.117 \times 10^{+07}$	SF
²⁹³ 119	15.317	0.139×10^{-08}	0.120×10^{-08}	0.596×10^{-09}	0.409×10^{-09}	0.185×10^{-09}	$0.468 \times 10^{+13}$	$\alpha 1$
$^{289}\mathrm{Ts}$	12.984	0.139×10 0.619×10^{-05}	0.120×10^{-05} 0.183×10^{-05}	$0.390 \times 10^{-0.05}$ $0.240 \times 10^{-0.05}$	$0.409 \times 10^{-0.5}$ $0.174 \times 10^{-0.5}$	0.133×10^{-06} 0.230×10^{-06}	$0.465 \times 10^{+08}$	$\frac{\alpha_1}{\alpha_2}$
$^{285}\mathrm{Mc}$	11.603	0.019×10^{-02} 0.160×10^{-02}	0.183×10^{-03} 0.248×10^{-03}	0.240×10^{-03} 0.577×10^{-03}	0.174×10 0.439×10^{-03}	0.250×10^{-04} 0.254×10^{-04}	$0.403 \times 10^{+04}$ $0.978 \times 10^{+04}$	
^{281}Nh		$0.656 \times 10^{+00}$	0.248×10^{-01} 0.556×10^{-01}	0.377×10 $0.223 \times 10^{+00}$	$0.439 \times 10^{+00}$ $0.178 \times 10^{+00}$	0.254×10 0.421×10^{-02}	$0.366 \times 10^{+02}$	$\alpha 3$
277 Rg	10.317	$0.384 \times 10^{+00}$	0.363×10^{-01}	$0.223 \times 10^{+00}$ $0.126 \times 10^{+00}$	$0.178 \times 10^{+00}$ $0.102 \times 10^{+00}$	0.421×10^{-02} 0.256×10^{-02}	$0.366 \times 10^{+01}$ $0.203 \times 10^{+01}$	$\alpha 4$
$^{273}\mathrm{Mt}$	$10.169 \\ 10.508$	0.384×10^{-01} 0.116×10^{-01}	0.363×10 0.161×10^{-02}	$0.126 \times 10^{-0.00}$ $0.371 \times 10^{-0.00}$	0.102×10^{-02} 0.299×10^{-02}	0.256×10 0.124×10^{-03}	$0.203 \times 10^{+01}$ $0.138 \times 10^{+01}$	$\alpha 5$
269 Bh		0.175×10^{-01} 0.175×10^{-01}	$0.101 \times 10^{-0.101}$ $0.118 \times 10^{+0.2}$	$0.571 \times 10^{-0.550} \times 10^{+0.2}$	$0.299 \times 10^{-0.02}$ $0.474 \times 10^{-0.02}$	0.124×10^{-00} 0.469×10^{-00}	$0.138 \times 10^{+01}$ $0.936 \times 10^{+01}$	$\alpha 6$
$^{265}\mathrm{Db}$	8.814	0.175×10 $0.178 \times 10^{+09}$	$0.118 \times 10^{+07}$ $0.658 \times 10^{+07}$	$0.550 \times 10^{+08}$ $0.578 \times 10^{+08}$	0.474×10 $0.553 \times 10^{+08}$	0.469×10 $0.678 \times 10^{+05}$	$0.936 \times 10^{+03}$ $0.512 \times 10^{+03}$	$rac{lpha7}{ ext{SF}}$
Ъб	6.833	0.178 × 10	0.038 × 10	0.378 × 10	0.555 × 10	0.078 × 10	0.312 × 10	SF
$^{294}119$	15.131	0.607×10^{-08}	0.218×10^{-08}	0.113×10^{-08}	0.135×10^{-08}	0.118×10^{-08}	$0.936 \times 10^{+10}$	$\alpha 1$
$^{290}\mathrm{Ts}$	12.956	0.155×10^{-04}	0.204×10^{-05}	0.261×10^{-05}	0.514×10^{-05}	0.914×10^{-06}	$0.143 \times 10^{+06}$	$\alpha 2$
$^{286}\mathrm{Mc}$	11.561	0.440×10^{-02}	0.303×10^{-03}	0.692×10^{-03}	0.192×10^{-02}	0.110×10^{-03}	$0.463 \times 10^{+02}$	$\alpha 3$
$^{282}\mathrm{Nh}$	10.188	$0.325 \times 10^{+01}$	$0.115 \times 10^{+00}$	$0.481 \times 10^{+00}$	$0.201 \times 10^{+01}$	0.300×10^{-01}	$0.267 \times 10^{+00}$	SF
$^{278}\mathrm{Rg}$	9.925	$0.398 \times 10^{+01}$	$0.148 \times 10^{+00}$	$0.570 \times 10^{+00}$	$0.228 \times 10^{+01}$	0.345×10^{-01}	0.229×10^{-01}	SF
205		10	10	10	10	10	1.07	
$^{295}119$	16.177	0.695×10^{-10}	0.868×10^{-10}	0.277×10^{-10}	0.187×10^{-10}	0.142×10^{-10}	$0.321 \times 10^{+07}$	$\alpha 1$
$^{291}{ m Ts}$	11.763	0.253×10^{-02}	0.372×10^{-03}	0.884×10^{-03}	0.663×10^{-03}	0.396×10^{-04}	$0.842 \times 10^{+02}$	$\alpha 2$
$^{287}{ m Mc}$	$11.332 \ (10.74)^*$	0.695×10^{-02}	0.918×10^{-03}	0.229×10^{-02}	0.176×10^{-02}	0.892×10^{-04}	0.469×10^{-01}	$\alpha 3$
^{283}Nh	10.097 (10.26)*	$0.581 \times 10^{+01}$	$0.194 \times 10^{+00}$	$0.859 \times 10^{+00}$	$0.375 \times 10^{+01}$	0.494×10^{-01}	0.468×10^{-03}	SF
$^{279}\mathrm{Rg}$	$9.666 (10.52)^*$	$0.221 \times 10^{+02}$	$0.697 \times 10^{+00}$	$0.315 \times 10^{+01}$	$0.143 \times 10^{+02}$	$0.150 \times 10^{+00}$	0.699×10^{-04}	SF
²⁹⁶ 119	16.017	0.262×10^{-09}	0.139×10^{-09}	0.455×10^{-10}	0.435×10^{-10}	0.803×10^{-10}	$0.192 \times 10^{+03}$	$\alpha 1$
$^{292}\mathrm{Ts}$	11.596	0.136×10^{-01}	0.822×10^{-03}	0.207×10^{-02}	0.662×10^{-02}	0.304×10^{-03}	0.963×10^{-02}	$\alpha 2/SF$
$^{288}\mathrm{Mc}$	11.262 (10.46)*	0.130×10^{-01} 0.225×10^{-01}	0.022×10^{-02} 0.130×10^{-02}	0.324×10^{-02}	0.101×10^{-01}	0.304×10^{-03} 0.443×10^{-03}	0.103×10^{-04} 0.103×10^{-04}	$\frac{\alpha z}{SF}$
$^{284}\mathrm{Nh}$	9.920 (10.00)*	$0.184 \times 10^{+02}$	$0.547 \times 10^{+00}$	$0.324 \times 10^{-0.00}$ $0.250 \times 10^{+0.00}$	$0.101 \times 10^{+02}$ $0.119 \times 10^{+02}$	$0.133 \times 10^{+00}$	0.103×10^{-06} 0.199×10^{-06}	SF
$^{280}\mathrm{Rg}$	9.454 (9.75)*	0.164×10 $0.943 \times 10^{+02}$	$0.260 \times 10^{+01}$	$0.124 \times 10^{+02}$	$0.622 \times 10^{+02}$	$0.521 \times 10^{+00}$	0.199×10 0.582×10^{-07}	SF
9	0.101 (0.10)							
$^{297}119$	16.034	0.113×10^{-09}	0.132×10^{-09}	0.413×10^{-10}	0.279×10^{-10}	0.215×10^{-10}	0.205×10^{-02}	$\alpha 1$
$^{293}\mathrm{Ts}$	11.251	0.419×10^{-01}	0.447×10^{-02}	0.134×10^{-01}	0.102×10^{-01}	0.439×10^{-03}	0.218×10^{-06}	SF
$^{289}\mathrm{Mc}$	11.181	0.161×10^{-01}	0.194×10^{-02}	0.489×10^{-02}	0.375×10^{-02}	0.183×10^{-03}	0.499×10^{-09}	SF
285 Nh	9.751	$0.259 \times 10^{+02}$	$0.151 \times 10^{+01}$	$0.743 \times 10^{+01}$	$0.602 \times 10^{+01}$	0.984×10^{-01}	0.209×10^{-10}	SF
$^{281}\mathrm{Rg}$	9.276	$0.151 \times 10^{+03}$	$0.810 \times 10^{+01}$	$0.418 \times 10^{+02}$	$0.347 \times 10^{+02}$	0.430×10^{00}	0.134×10^{-10}	SF

Another formula for α —decay half-lives based on generalized liquid drop model proposed by Dasgupta-Schubert and Reyes [42] is obtained by fitting the experimental half-lives for 373 alpha emitters, given as

$$\log_{10} T_{\frac{1}{2}}^{\alpha} = a + bA^{1/6}Z^{1/2} + cZ/Q_{\alpha}^{1/2}. \tag{22}$$

The parameters a, b and c are given by

$$a,b,c = \begin{cases} -25.31, -1.1629, 1.5864 \ even - even; \\ -26.65, -1.0859, 1.5848 \ even - odd; \\ -25.68, -1.1423, 1.5920 \ odd - even; \\ -29.48, -1.1130, 1.6971 \ odd - odd \ . \end{cases} \tag{23}$$

Recently, in Ref. [43] Ni et. al. proposed a unified formula for determining the half-lives in alpha decay and cluster radioactivity. The formula for alpha decay is written as

$$\log_{10} T_{1/2}^{\alpha} = 2a\sqrt{\mu}(Z-2)Q_{\alpha}^{-1/2} + b\sqrt{\mu}[2(Z-2)]^{-1/2} + c$$
(24)

where, a, b, c are the constants and μ is define as 4(A-4)/A.

3.5.2 Beta decay

Beta decay, a three body decay mode, is another very important mode of decay for the nuclei lie far from the stability line. The description of β -decay is explained by famous Fermi theory which describes the beta transition rates according to log(ft) values. It proceeds through weak interaction and this process is slow as well as less favoured compared to SF and alpha decay. Recently, it is predicted that there may also be a possibility of β -decay in some of the superheavy nuclei where it may play a significant role [103]. In this regard, even in the presence of dominant mode of alpha and SF in SHN, we make the search for possibility of β -decay in order to completeness of decay modes of superheavy nuclei. To look out the possibility of β -decay in considered isotopic chain, we employed the empirical formula of Fiset and Nix [102] for estimating the half-lives of the isotopic chain under study which is given by

$$T_{1/2}^{\beta} = 540 \times 10^{5.0} \frac{m_e^5}{\rho_{d.o.s.}(W_{\beta}^6 - m_e^6)}.$$
 (25)

In an analogy of α -decay, we evaluate the Q_{β} value using the relation $Q_{\beta} = BE(Z+1,A) - BE(Z,A)$ and further we calculate the W_{β} by a relation $W_{\beta} = Q_{\beta} + m_e$, where, m_e is the rest mass of electron. Here, $\rho_{d.o.s.}$ is the average density of states in the daughter nucleus $(e^{-A/290} \times \text{number of states})$ within 1 MeV of ground state).

3.5.3 Spontaneous Fission

Superheavy nuclei are identified by alpha decay and the chain ends by spontaneous fission which helps in identifying the long lived superheavy elements. Several empirical formulas for determining the spontaneous fission half-lives are available in literature proposed by various authors from time to time. In our calculations, we employed

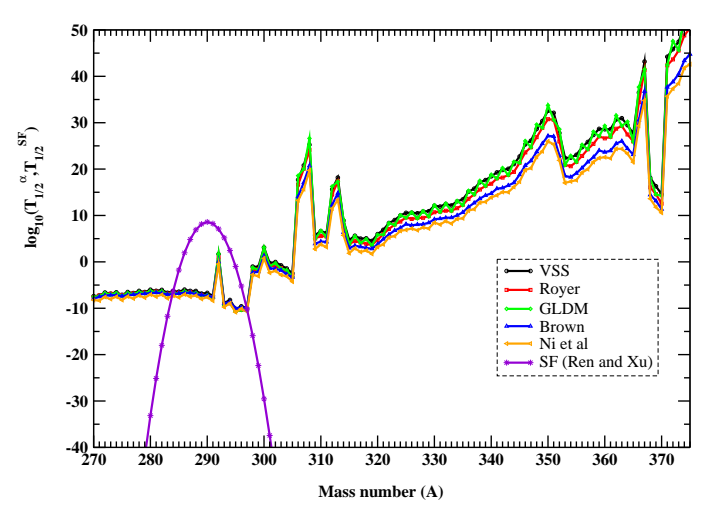


Fig. 5. (color online) Alpha decay and spontaneous fission half-lives of Z=119 isotopic chain as a function of mass number

the phenomenological formula proposed by Ren and Xu [61] as expressed by

$$\log_{10} T_{1/2}^{SF} = 21.08 + C_1 \frac{(Z - 90 - \nu)}{A} + C_2 \frac{(Z - 90 - \nu)^2}{A} + C_3 \frac{(Z - 90 - \nu)^3}{A} + C_4 \frac{(Z - 90 - \nu)(N - Z - 52)^2}{A}, \tag{26}$$

where Z, N, A represent the proton, neutron and mass number of parent nuclei. The values of empirical constants are C_1 =548.825021, C_2 =5.359139, C_3 = 0.767379, C_4 =4.282220 [62]. The quantity ν is the seniority term which is 0 for the spontaneous fission of even-even nuclei and 2 for spontaneous fission of odd-A nuclei.

Present analysis shows that some of the isotopes of Z = 119 superheavy nuclei survived the fission and thus make the decay via $\alpha-$ emission. The calculated $\alpha-$ decay half-lives using VSS, Brown, Royer, GLDM and Ni et al. are framed in Tables 3, 4 and we noticed a good agreement among them as well as with FRDM data. Fiset and Nix formula is employed to calculate the β -decay half-life for examining the possibility of mode of β -decay and the results are also presented in Tables 3 and 4. It is noted that β -decay half-lives are found to be large than α -decay as well as spontaneous fission half-lives and hence there is no possibility of mode of β -decay is observed for current isotopic chain. Spontaneous fission half-lives is calculated using Ren and Xu formula and the estimated values are framed in one of the columns of Tables 3-6. The calculated half-lives for α -decay and SF are plotted against the mass number displayed in Fig. 5.

Our calculations predict that the nuclides $^{284-297}119$ survive the fission and may be observed in the laboratory through alpha decay and the nuclei beyond A > 297 do not survive fission and hence completely undergo spontaneous fission. Further, we aimed at predicting the pos-

sibility of α -decay chain of fission survival nuclides i.e. ^{284–297}119 of the considered isotopic chain given in Table 3. Our study confirmed the possibility of one α chain from $^{297}119$, two consistent α chains from $^{284,285,296}119$, three consistent α chains from $^{294,295}119$, four consistent α chains from $^{285}119,$ five consistent α chains from $^{286}119,$ seven consistent α chains from $^{287,292,293}119$ and nine cons sistent α chains from $^{288,289,290,291}119$ and these findings are reported in the Tables 5 and 6. Unfortunately, there is no experimental information for Z = 119 nuclides. But the experimental data of Q_{α} for a few decay elements of Z = 119 is available [104, 105, 106] and we mentioned in Tables 5 and 6. The calculated values of Q_{α} are compared with available experimental data [104, 105, 106] and we found a close agreement between them. Moreover, the α -decay chain of ²⁹⁵119 contains ²⁹¹Ts, ²⁸⁷Mc, ²⁸³Nh and ^{279}Rg elements whose α -decay chain is treated in Refs. [84, 107] and a close agreement of our calculated Q_{α} with the values predicted in these Refs. [84, 107] is noticed. However, we did not mention the values of Q_{α} predicted in Refs. [84, 107] into the manuscript. The inference drawn from this investigations is that the nuclides $^{284-297}119$ have the α -decay chain with the life-time of the order of micro- or nano-second and thus these nuclides might be observed in the laboratory through alpha decay. We firmly believed that the alpha decay life-time of the isotopes $^{284-297}119$ presented in the manuscript may serve as a crucial theoretical input for designing the experimental setup and might provide a ray of hope in order to produce the vet-to-be synthesized isotopes of Z=119 in the laboratory in very near future.

4 Summary

In summary, we have calculated the structural properties of Z = 119 superheavy nuclei within a mass range $284 \le A \le 375$ using axially deformed relativistic mean field model. The calculations are performed for three different shape configurations prolate, oblate and spherical configurations in which prolate is suggested to be possible ground state for most of the nuclei. Binding energy produced by RMF are in good agreement with FRDM data. Two dimensional contour plot of density distribution has been made for predicting neutron shell closure nuclides $^{291}119$ and $^{303}119$ to reveal the special features of the nuclei such as bubble or cluster structures. Further, the predictions of possible modes of decay such as α -decay, β -decay and spontaneous fission of the isotopic chain of Z=119 in the mass range $284 \le A \le$ 375 have been made. The calculations performed for α decay half-lives using the semi-empirical formulae Viola-Seaborg, Brown, Royer, GLDM and Ni et. al. are in good agreement with among each other as well as with macromicroscopic FRDM data wherever available. In addition, a thorough study on β -decay and SF half-lives have also been made to identify the mode of the decay of these isotopes. We conclude that the α -decay and spontaneous fission are the principal modes of decay in considered chain of nuclides and there is no possibility of β -decay for the considered chain of nuclides under study. The calculated values of Q_{α} are compared with experimental data [104, 105, 106], wherever available and found a close agreement between them. Moreover, our calculated Q_{α} are quite agreeable with the values predicted in Refs. [84, 107]. From our analysis we inferred that the isotopes with mass number $284 \le A \le 297$ will survive fission and can be observed in the laboratory through alpha decay while beyond the mass number A > 297 do not survive fission and hence completely undergoes spontaneous fission. We also analyzed the α -decay chain of fission survival nuclides i.e. ^{284–297}119 for the considered isotopic chain and predicted one α decay chain, two consistent α decay chains, three consistent α decay chains, four consistent α decay chains, five consistent α decay chains, seven consistent α decay chains and nine consistent α decay chains. Findings suggest that the nuclides $^{284-297}119$ have α -decay chains and thus these nuclides might be observed in the laboratory through alpha decay. We hope that the predictions on the possible decay modes of Z = 119 superheavy nuclei might prove to be quite useful and may serve as a significant input for future experimental investigations.

5 Acknowledgments

One of the authors (M.I.) would like to acknowledge the hospitality provided by the Institute of Physics, Bhubaneswar where a piece of this work was carried out. M.I. gratefully acknowledges the financial support in the form of research associate fellowship from the Council of Scientific and Industrial Research (CSIR), Government of India.

References

- S. C. Cwiok, J. Dobaczewski, P.-H. Heenen, P. Magierski, and W. Nazarewicz, Nucl. Phys. A 611, 211 (1996).
- 2. W. D. Myers, W. J. Swiatecki, Nucl. Phys. A 81, 1 (1966).
- A. Sobiczewski, F. A. Gareev, B. N. Kalinkin, Phys. Lett. 22, 500 (1966).
- 4. U. Mosel, W. Greiner, Z. Phys. 222, 261 (1969).
- S. C. Cwiok, V. V. Pashkevich, J. Dudek, W. Nazarewicz, Nucl. Phys. A 41, 254 (1983).
- 6. Z. Patyk, A. Sobiczewski, Nucl. Phys. A 533, 132 (1991).
- S. Hoffman, G. Munzenberg, Rev. Mod. Phys. 72, 733 (2000).
- Yu.Ts. Oganessian, J. Phys. G: Nucl. Part. Phys. 34, R165 (2007).
- S. Hofmann, F.P. Heberger, D. Ackermann, S. Antalic, P. Cagarda, B. Kindler, P. Kuusiniemi, M. Leino, B. Lommel, O.N. Malyshev, R. Mann, G. Munzenberg, A.G. Popeko, S. Saro, B. Streicher, A.V. Yeremin, Nucl. Phys. A 734, 93 (2004).
- 10. D. Ackermann, Nucl. Phys. A **787**, 353c (2007).
- 11. K. Morita, Nucl. Phys. A 944, 30 (2015).
- Yu.Ts. Oganessian, V.K. Utyonkov, Rep. Prog. Phys. 78, 036301 (2015).
- 13. Yu.Ts. Oganessian et al., Phys. Rev. C **79**, 024603 (2009).

- Yu. Ts Oganessian et. al., Phys. Rev. Lett 109, 162501 (2012).
- Yu. Ts. Oganessian et al., JINR Communication No. E7-2012-58, (2012).
- J. C. Pei, F. R. Xu, Z. J. Lin, and E. G. Zhao, Phys. Rev. C 76, 044326 (2007).
- M. M. Sharma, A. R. Farhan, and G. Munzenberg, Phys. Rev. C 71, 054310 (2005).
- 18. W.D. Myers, W.J. Swiatecki, Ark. Fys. 36, 343 (1967).
- 19. H. Meldner, Ark. Fys. 36, 593 (1967).
- S. G. Nilsson, C. F. Tsang, A. Sobiczewski, Z. Szymanski, S. Wycech, C. Gustafson, I. L. Lamm, P. Möller, B. Nilsson, Nucl. Phys. A 131, 1 (1969).
- R. K. Gupta, S. K. Patra and W. Greiner, Mod. Phys. Lett. A 12, 1727 (1997).
- S. K. Patra, Cheng-Liwu, C. R. Praharaj and R. K. Gupta, Nucl. Phys. A 651, 117 (1999).
- M. Bhuyan and S. K. Patra, Mod. Phys. Lett. A 27, 1250173 (2012).
- M. Bender, K. Rutz, P.G. Reinhard, J.A. Maruhn, W. Greiner, Phys. Rev. C 58, 2126 (1998).
- K. Rutz, M. Bender, T. Burvenich, T. Schilling, P.G. Reinhard, J.A. Maruhn, W. Greiner, Phys. Rev. C 56, 238 (1997).
- T. Sil, S.K. Patra, B.K. Sharma, M. Centelles, X. Viñas, Phys. Rev. C 69, 044315 (2004).
- S. Cwiok, W. Nazarewicz, and P. H. Heenen, Phys. Rev. Lett. 83, 1108 (1999).
- J. Dong, W. Zuo, and W. Scheid, Phys. Rev. Lett. 107, 012501 (2011).
- D. N. Poenaru, R. A. Gherghescu, and W. Greiner, Phys. Rev. Lett. 107, 062503 (2011).
- E. Rutherford, H. Geiger, Proc. R. Soc. Lond. Ser. A 81, 162 (1908).
- 31. E. Rutherford, T. Royds, Philos. Mag. 17, 281 (1909).
- 32. G. Gamow, Z. Phys. 51, 204 (1928).
- B. Buck, A. C. Merchant, and S. M. Perez, Phys. Rev. C 45, 2247 (1992).
- 34. D. N. Poenaru, M. Ivascu, A. Sandalescu, and W. Greiner, Phys. Rev. C 32, 572 (1985).
- 35. D. N. Basu, Phys. Lett. B 566, 90 (2003).
- 36. H. F. Zhang and G. Royer, Phys. Rev. C 76, 047304 (2007).
- Y.Z. Wang, S.J. Wang, Z.Y. Hou, J.Z. Gu, Phys. Rev. C 92, 064301 (2015).
- 38. Asloob A. Rather, M. Ikram, A. A. Usmani, Bharat Kumar, and S. K. Patra, Eur. Phys. J. A, **52**, 372 (2016).
- V. E. Viola, Jr. and G. T. Seaborg, J. Inorg. Nucl. Chem. 28, 741 (1966).
- 40. G. Royer, J. Phys. G, Nucl. Part. Phys. 26, 1149 (2000).
- 41. B. A. Brown, Phys. Rev. C 46, 811 (1992).
- N. Dasgupta-Schubert and M. A. Reyes, At. Data Nucl. Data Tables 93, 90 (2007).
- 43. D. D. Ni , Z. Z. Dong, and T. K et al. Phys. Rev. C, **78**, 044310 (2008).
- N. Wang, M. Liu, X.Z. Wu, J. Meng, Phys. Lett. B 734, 215 (2014).
- D.N. Poenaru, R.A. Gherghescu, N. Carjan, EPL 77, 62001 (2007).
- V.E. Viola, jr., G.T. Seaborg, J. Inorg. Nucl. Chem. 28, 741 (1966).
- A. Sobiczewski, Z. Patyk, S. C. Cwiok, Phys. Lett. B 224, 1 (1989).

- 48. A. Sobiczewski, A. Parkhomenko, Prog. Part. Nucl. Phys. 58, 292 (2007).
- A. Parkhomenko, A. Sobiczewski, Acta Phys. Pol. B 36, 3095 (2005).
- D. Ni, Z. Ren, T. Dong, C. Xu, Phys. Rev. C 78, 044310 (2008).
- 51. N. Bohr and J. A. Wheeler, Phys. Rev. **56**, 426 (1939).
- 52. G.N. Flerov, K.A. Petrjak, Phys. Rev. 58, 89 (1940).
- 53. W.J. Swiatecki, Phys. Rev. 100, 937 (1955).
- 54. Yu.Ts. Oganessian et. al., Phys. Rev. C 72, 034611 (2005).
- 55. Yu.Ts. Oganessian, et. al., Phys. Rev. C 74, 044602 (2006).
- K.E. Gregorich, J.M. Gates, Ch.E. Dullmann, R. Sudowe, S.L. Nelson, M.A. Garcia, I. Dragojevi, C.M. Folden III, S.H. Neumann, D.C. Hoffman, H. Nitsche, Phys. Rev. C 74, 044611 (2006).
- 57. J. Dvorak et. al., Phys. Rev. Lett. 97, 242501 (2006).
- 58. D. Peterson et. al., Phys. Rev. C 74, 014316 (2006).
- 59. Yu.Ts. Oganessian et. al., Phys. Rev. C 70, 064609 (2004).
- 60. C. Xu, Z. Ren, Y. Guo, Phys. Rev. C 78, 044329 (2008).
- 61. Z. Ren, C. Xu, Nucl. Phys. A **759**, 64 (2005).
- 62. C. Xu, Z. Ren, Phys. Rev. C **71**, 014309 (2005).
- R. Smolanczuk, J. Skalski, A. Sobiczewski, Phys. Rev. C 52, 1871 (1995).
- I. Muntain, Z. Patyk, A. Sobiczewski, Acta Phys. Pol. B 34, 2141 (2003).
- 65. M. Warda, J.L. Egido, Phys. Rev. C 86, 014322 (2012).
- A. Staszczak, A. Baran, W. Nazarewicz, Phys. Rev. C 87, 024320 (2013).
- W. Pannert, P. Ring and J. Boguta, Phys. Rev. C 59, 2420 (1987).
- 68. B. D. Serot, Rep. Prog. Phys. 55, 1855 (1992).
- Y. K. Gambhir, P. Ring, and A. Thimet, Ann. Phys. (N.Y.) 198, 132 (1990).
- 70. P. Ring, Prog. Part. Nucl. Phys. 37, 193 (1996).
- B. D. Serot and J. D. Walecka, Adv. Nucl. 16, 1 (1986).
- J. Boguta, and A. R. Bodmer, Nucl. Phys. A 292, 413 (1977).
- S. K. Patra and C. R. Praharaj, Phys. Rev. C 44, 2552 (1991).
- Z. Ren, D. H. Chen, F. Tai, H. Y. Zhang and W. Q. Shen, Phys. Rev. C 76, 064302 (2003).
- M. M. Sharma and A. R. Farhan, Phys. Rev. C 71, 054310 (2005).
- 76. D. G. Madland, R. J. Nix, Nucl. Phys. A 476, 1 (1988).
- G. A. Lalazissis, J. Konig and P. Ring, Phys. Rev. C 55, 510 (1997).
- Yu. Ts. Oganessian et. al., Phy. Rev. Lett. 74, 044602 (2006).
- Yu. Ts. Oganessian, J. Phys. G: Nucl. Part. Phys. 34, R165 (2007).
- 80. Z. H. Liu and J. D. Bao, Phys. Rev. C 80, 054608 (2009).
- N. Ghahramany and A. Ansari, Eur. Phys. J. A 52, 287(2016).
- N. Wang, E. G. Zhao, W. Schield and S. G. Zhou, Phys. Rev. C 85, 041601(R) (2012).
- L. Zhu, W. J. Xie and F. S. Zhang, Phys. Rev. C 89, 024615 (2014).
- G. G. Adamian, N. V. Antoneko and H. Lenske, Nucl. Phys. A 970, 22 (2018).
- G. Z. Guo, Z. X. Hong, H. M. Hui, F. Z. Qing, L. J. Qing, Science China 54, s61 (2011).
- P. Möller, J. R. Nix, W. D. Wyers, and W. J. Swiatecki,
 At. Data Nucl. Data Tables 59, (1999) 185; P. Möller, J.
 R. Nix and K. L. Kratz *ibid*, 66, 131 (1997).

- 87. H. Morinaga, Phys. Rev. 101, 254 (1956).
- 88. P. Van Duppen, E. Coenen, K. Deneffe, M. Huyse, K. Heyde, and P. Van Isacker, Phys. Rev. Lett **52** 1974 (1984).
- 89. A. N. Andreyev et al., Nature **405**, 430 (2000).
- 90. Z. Ren, Phys. Rev. C, 65 051304(R) (2002).
- 91. Z. Shi-Jie, X. Fu-Rong, Chin. Phys. C, **32** (2008).
- Z. X. Li, Z. H. Zhang, and P. W. Zhao, Front. Phys. 10, 102101(2015).
- S. Ćwiok, P. H. Heenen, W. Nazarewicz, Nature 433, 705 (2000).
- 94. Z. Ren, H. Toki, Nucl. Phys. 689, 691 (2001).
- 95. J. A. Wheeler (unpublished).
- 96. H. A. Wilson, Phys. Rev. C 69, 538 (1946).
- 97. J. Decharge et. al., Nucl. Phys. A **716**, 55 (2003).
- 98. M. Grasso et. al., Phys. Rev. C 79, 034318 (2009).
- S. K. Singh, M. Ikram and S. K. Patra, Int. J. Mod. Phys. E 22, 1350001 (2013).
- 100. B. K. Sharma, P. Arumugam, S. K. Patra, P. D. Stevenson, R. K. Gupta and W. Greiner, Phys. G: Nucl. Part. Phys. **32**, L1 (2006).
- G. Audi, A. H. Wapstra and C. Thibault, Nucl. Phys. A 729, 337 (2003).
- 102. E. O. Fiset and J. R. Nix, Nucl. Phys. A 193, 647 (1972).
- 103. A. V. Karpov and V. I. Zagrebaev, Int. J. Mod. Phys. E 21, 1250013 (2012).
- 104. Yu. Ts. Oganessian, J. Phys. G 34, R165 (2007).
- 105. Yu. Ts. Oganessian, Phys. Rev. C 87, 014302 (2013).
- 106. J. H. Hamilton, Yu. Ts. Oganessian and V. K. Utyonkov et. al., J. Phys. G: Conf. series 403, 012035 (2012).
- 107. A. N. Kuzmina, G. G. Adamian and N. V. Antonenko, Phys. Rev. C 85, 017302 (2012).